# MOLECULAR MODELLING - THE ROLE OF ZINC ION IN TRANSITION STATE OF CLASS B β-LACTAMASE HYDROLYSIS OF PENICILLINS.

by

**Manish Dhawan**

Submitted in Partial Fulfillment of the Requirements

For the Degree of

Master of Science

In the

Chemistry

Program

**YOUNGSTOWN STATE UNIVERSITY**
May, 2007

**Molecular Modeling- The Role of Zinc ion in Transition State of class B β-Lactamase Hydrolysis of penicillins**

Manish Dhawan

I hereby release this thesis to the public. I understand that this thesis will be housed at the Circulation Desk of the University library and will be available for public access. I also authorize the University or other individuals to make copies of this thesis as needed for scholarly research.

Signature; Manish Dhawan May 15th 2007

Manish Dhawan Date

Approvals;

Howard Mettee May 9 2007

Dr.Howard Mettee, Thesis Advisor Date

Timothy R. Wagner May 15 2007

Dr.Timothy R.Wagner, Committee Member Date

Michael A. Serra May 15, 2007

Dr.Michael A.Serra, Committee Member Date

Peter J. Kasvinsky May 16, 2007

Dr. Peter J. Kasvinsky, Dean of Graduate Studies Date

## Abstract

The focus of this research is computational work on the initial, transition and final state of class B β- lactamase hydrolysis of penicillin and the role of zinc ions with various theoretical models using a variety of basis sets. The model includes semi-empirical, Hartree-Fock (HF), and density functional (DFT), and MP2 (Moller Plesset) theory in the Spartan Pro$^{TM}$, 2004$^{TM}$ program suite. The role of zinc ions in β- lactamase enzyme was reflected by observing its effects on reducing the activation energies. Activation energies were computed for β- lactam ring, β- lactam thiol ring, benzyl Penicillin and various transition state complexes involved in concerted reaction, both with and without zinc ions. The corresponding values are for β- lactam ring (7.88 to 56.72), β- lactam thiol ring (18.10 to 69.10), and benzyl Penicillin (11.87 to 13.16) kcal/mol of reduction in $E_a$ due to zinc ions, with different levels of semi-empirical, Hartree-Fock, and density functional theories and complexity of the mechanism. A simplified mimic of the active site was optimized by different levels of theory and the geometry of it was in accord, with that found by X-ray diffraction experiments of the crystal.

## Acknowledgements

I would like to thank Professor Howard Mettee for supervising this project and for his devoted guidance during the period of this project, especially his suggestions and corrections of the thesis which made it successful. And I would like to thank Professors Timothy R. Wagner and Micheal A. Serra for being on my thesis committee. Special thanks are also due to the Chemistry Department and faculty for their guidance and support to pursue my masters. In additional I would like to thank my parents, my wife, my two beautiful kids and Vivek in giving me inspiration to pursue my master degree, and in last but not least I would like to thank my friends Daryl, Calvin, Naresh for their moral support.

# Table of Contents

Page

## Table of Contents (cont'd)

## Table of Contents (cont'd)

## List of Tables:

Page

# Table of Figures:

# List of Abbreviations

| | |
|---|---|
| AM1 | Austin model1, a semi-empirical method |
| B3LYP | A density functional method due to Lee, Yang and Parr |
| DFT | Density functional theory |
| EWG | Electron withdrawing group |
| HF | Hartfree-Fock method |
| HOMO | Highest occupied molecular orbital |
| LDA | Local density approximation |
| LUMO | Lowest unoccupied molecular orbital |
| MNDO | Modified neglect of diatomic overlap |
| PM3 | Parameterized model 3, a semi-empirical method |
| $\Delta G^0$ | Standard free energy change between reactants and products |
| $\Delta H^0$ | Standard enthalpy change between reactants and products |
| $\Delta S^0$ | Standard entropy change between reactants and products |
| $\Delta G^\dagger$ | Free energy change between reactants and transition state |
| $\Delta H^\dagger$ | Enthalpy change between reactants and transition state |
| $\Delta S^\dagger$ | Entropy change between reactants and transition state |
| R | Universal gas constant |
| k | Boltzmann constant |
| h | Planck constant |
| STO-3G | Slater type orbital's in terms of three Gaussians |
| 3-21G | Split valence basis set using three Gaussians for inner shell orbitals |

| | |
|---|---|
| 6-21G | Split valence basis set using six Gaussians for inner shell orbitals |
| 6-31G* | Split valence basis set with d-orbitals |
| 6-31G** | Split valence basis set 6-31G* with additional P-orbitals |
| $K_e$ | Equilibrium constant between reactants and products |
| $K^{\ddagger}$ | Equilibrium constant between reactants and transitional state |

# CHAPTER 1

## 1) Introduction

It is over seventy years since Alexander Fleming observed antibiosis between a Penicillium mould and bacterial cultures, and gave the name Penicillin to the active principle[1]. Although it was proposed in 1943 that Penicillin contained a β- lactam ring, this was not generally accepted until an X-ray crystallographic determination of the structure had been completed[1]. Penicillin was the first naturally occurring antibiotic to be characterized and used in clinical medicine. It is now seen as the progenitor of the β- lactam family of antibiotics, which are characterized by the possession of the four membered β- lactam rings[2].

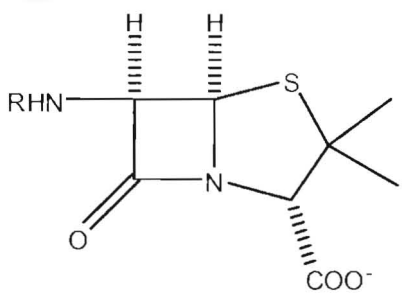


**Figure 1: General skeleton of Penicillin[2]**

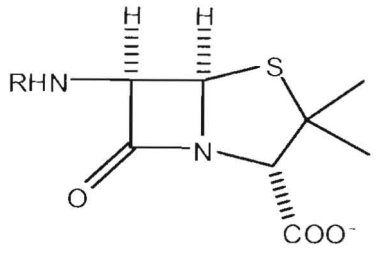


| | R | Name |
|---|---|---|
| 1 | 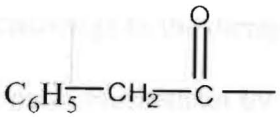 | Benzylpenicillin |
| 2 | 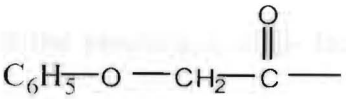 | Phenoxymethylpenicillin |
| 3 | 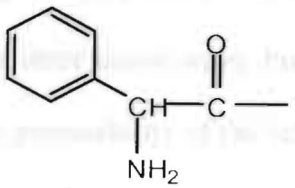 | Ampicillin |
| 4 | 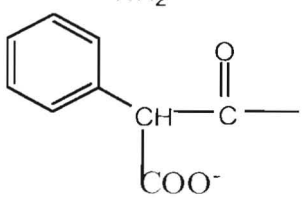 | Carbenicillin |
| 5 | 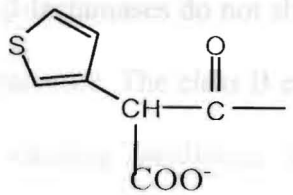 | Ticarcillin |
| 6 |  | Cloxacillin |

**Figure 2: Penicillin structural types[2]**

The increase in resistance to β-lactam antibiotics and the production of metallo-β-lactamases in pathogenic bacteria demonstrate the increased potential they have in reducing the effectiveness of these powerful antibiotics. Therefore, it is widely accepted that the emergence of antibiotic resistance mediated by zinc- β- lactamases comprises an increasing challenge to the therapeutic future of β- lactam antibiotics[2].

The main mechanism by which bacteria develop resistance to β- lactam antibiotics involves of the production of β- lactamases, enzymes that inactivates the antibiotics by hydrolyzing the C-N bond of the β- lactam ring[2]. Bacteria develop antibiotic resistance strategies in three major ways. Production of hydrolytic enzymes known as β- lactamases, changes the permeability of the cell membrane and alterations of the target enzymes[3].

The β-lactamases identified so far fall into four classes according to the homology of their amino acids sequences. Class A, C and D use a serine dependent mechanism, while in class B β-lactamases, zinc ions participate in β- lactam cleavage[2].

Zinc β-lactamases do not share any sequence or structure similarity with active site serine β- lactamases. The class B enzymes have been realized as a real threat to the future efficacy of existing antibiotics because of their broad substrate profiles including Penicillins, Cephalosporins and the recently introduced carbapenems, and their increasing incidence among clinically important serine enzymes are ineffective against them. In *B. cereus* enzyme, the two zinc ions are ligated by active site residues that are generally conserved in all known B1 metallo- β- lactamases sequences. One zinc ion is coordinated by three histidines and a water molecule in a tetrahedral arrangement. The second zinc binding site contains an aspartate, a cysteine, a histidine, water molecule first and second molecule. The resulting coordination environment for second zinc is a distorted trigonal

bipyramidal arrangement[5]. Despite the relatively large number of known X-rays structures, the mode of action of class B β- lactamases remains unclear.

Our work concentrates on the reaction mechanism involved in the hydrolysis of the β-lactam ring on the role zinc 1 ion in the mechanism by applying quantum mechanical models of the active sides of β- lactamases. Various basis sets and theoretical methods will be evaluated for the accuracy and efficiency in predicting reaction pathways.

The goals of this research are to build the transition state of Penicillin and scale this up to PM3, B3LYP, and HF levels of theory, and evaluate the activation energies with and without zinc ions at these different levels of theories.

## 1a) Modeling Introduction

The use of modern molecular orbital theories to model actual chemical reactions has become increasingly possible due principally to advances in the sophistication and capacity of today's software and desktop computers[6]. This project is presented as a series of molecular calculations including these based on mechanical and quantum mechanical molecular orbital calculations including molecular mechanics, semi-empirical, density functional theory and electron correlation methods as they are included in the Spartan Pro,® Spartan 2004® suites of programs available from Wave Function, Inc. The computer used was Dell OPTIPILEX GX-270 Pentium-4. These methods have their origins in the well known Schrodinger equation, which predicts the energy in a system of attractively and repulsively interacting particles such as found in typical molecules, but the

mathematical details of the Hamiltonian operators and representative eigenfunctions need not be proposed by the program user, as they are contained in the modeling software.

It is normally sufficient to graphically describe the molecules or radicals/ions using ordinary bonding theories, and then specify a method and a type of orbital approximation in order to develop energy, enthalpy and entropy characteristics of a molecule (or transition state). Secondary features like electron polarization, dipole moments, and orbital symmetries may also be solved for along with numerous other useful properties[7].

Molecular mechanics assemblies are connected by springs (with characteristic force constants) acting as bonds between them in their familiar geometry, based on the previously known and accepted values for bond length, angles and strengths. This is perhaps the most primitive form of theory since there are no provisions to account for individual atomic nuclei and electrons, only their collective behaviors as atoms[7].

For each method of investigation, the modeling procedure is the same. First the molecule is constructed atom by atom, the positions being prompted by the program and the basis set is chosen, along with the properties desired and the calculation is started. When convergence of the energy is reached in an energy minimization, (an iterative process involving subtle adjustments of bond distances and angles), then the equilibrium geometry and other properties can be calculated (vibrational frequencies for example). Finally, the results must be critically analyzed, not only to understand the properties themselves, but also to see that the calculation has been performed correctly[7].

## 1b) β- Lactamase Active Site;

The structure of zinc dependent β- lactamase from *Bacillus cereus* has been determined at 1.9 Å resolutions in a crystal form with two molecules in the asymmetric unit and 400 waters. The active site contains two zinc ions: Zn 1 is tightly coordinated by His 86, His 88 and His 149, while Zn 2 is loosely coordinated by Asp 90, Cys 168, and His 210. In the transition state, with the β- lactam ring of penicillin included, for which we have no X-ray structural information, Wat1 is postulated to take in the hydrolysis (closest to β-lactam ring ) and Wat 2 probably replaces it in the following cycles. Zn1 is closest to β-lactam and helps change the polarization of the transition state, while the more remote Zn 2 may help bring Wat 2 to reaction center[3].

The starting structure was prepared from the 1.90 Å crystal structure of the *B-cereus* enzyme in binuclear form. The crystallography structure contains 2 enzyme molecules in an asymmetric unit and 400 crystallographic waters.

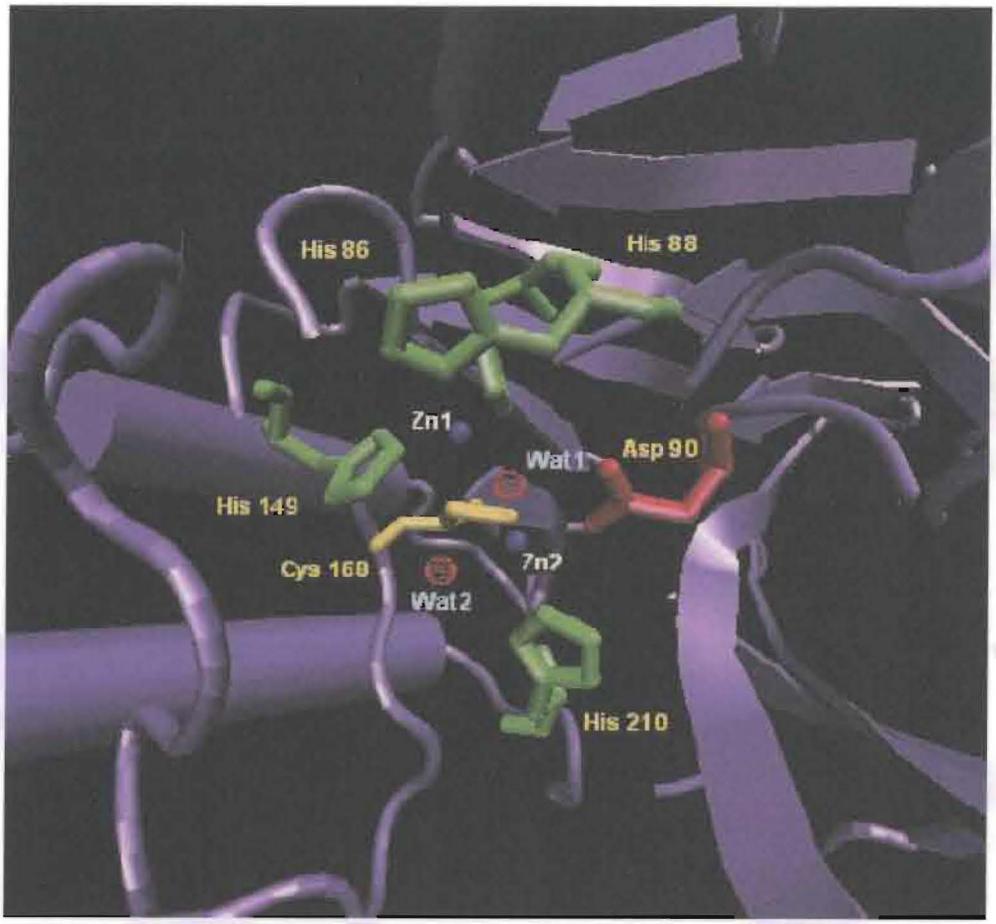


**Figure 3:** Structure of the active site of *Bacillus cereus* zinc β- lactamase.[10]

In figure 3 schematic representation of the hydrogen bonding network between the zinc ions and their direct and indirect ligands in the native enzyme model.

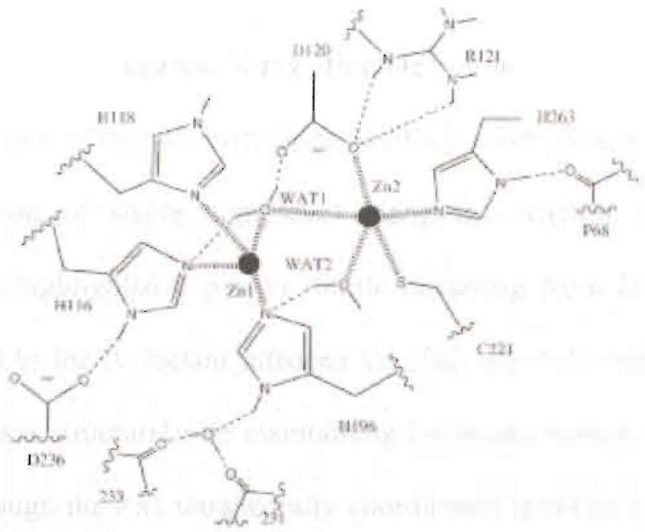


**Figure 4:** Schematic representation of the hydrogen-bonding network between the zinc ions and their direct and indirect ligands in the native enzyme model.[3]

## 1c) Literature review:

Barrie W. Bycroft and Richard E.Shute[8] investigated the molecular basis for the mode of action of β- lactam antibiotics and mechanisms of resistance and divided it into three sections. First, a brief introduction to the β- lactam antibiotic is presented from the stand point of their natural product origins. The second section is concerned with the bacterial cell wall structure and its biosynthesis, and the mode of action of β- lactam antibiotics. The final part covers the phenomenon of bacterial resistance to β- lactam antibiotic therapy and deals with the two most important manifestations of resistance; cell wall permeability and the production of β- lactamases.

C. Prosperi-Meys, J. Wouters[3] et al., studied the substrate binding and catalytic mechanism of class B β- lactamases. X-ray structures of several zinc β- lactamases have revealed the coordination of the two metal ions, but their mode of action remained unclear. Geometry optimization of stable complexes along the reaction pathway of benzyl Penicillin hydrolysis highlighted a proton shuttle occurring from D120 of the *Bacillus cereus* β- lactamases to the β- lactam nitrogen via Zn2 which is central to the network. First, the Zn1 ion has a structural role maintaining Zn-bound waters, WAT1 and WAT2, either directly or through the Zn1 tetrahedrally coordinated histidine ligands. The Zn2 ion has an extended catalytic role, both stabilizing the tetrahedral intermediate, accepting the β-lactam nitrogen atom as a ligand. The role of Zn2 and the flexibility in the coordination geometry of both Zn ions is of crucial importance for catalysis.

Natalia Diaz, Dimas Suarez[9] and co-workers studied the molecular dynamic simulations of the mononuclear β- lactamase from the *Bacillus cereus* complexed with benzyl Penicillin and a quantum chemical study of the reaction mechanism. The structural and dynamic effects induced by substrate-binding, the specific role of the conserved residues, and the near attack of the conformers of the Michaelis complex are discussed. Quantum chemical methods (HF/6-31G* and B3LYP/6-31G*) were also applied to study the hydrolysis reaction of N-methylaetidinone catalyzed by a monozinc system consisting of the side chains of the histidine residues(His86, His88, His149) complexed with Zn-OH and the side chains of Asp90 and His210. They proposed that the experimental rate data for the *B. cereus* enzyme is compatible with a one-step mechanism for the hydrolysis of β-lactam substrates in which His210 acts as a proton donor.

## 2) Computational methods:

The transition state energies of the β-lactam were calculated using semi-empirical, Hartree-Fock, density functional levels theory and other methods were performed at the AM1 and PM3 levels. The modeling system that was used in the Spartan 04™ for the geometries of the transition state as well as to obtain reaction energies (thermodynamics) and the activation energies (kinetics). The general procedure was to construct the reactant and product molecules followed by specifying the type of calculations (semi-empirical, etc.). The program adjusts the molecules geometry to minimize the energy, at which point the thermodynamic parameters (ΔH, ΔS) are generated from the moments of inertia, normal vibrational modes and columbic effects of electrons surrounding a frozen nuclear skeleton. Hartree-Fock and density functional theory was used for equilibrium and transition state structure determination as well as energy calculations.

## 2a) Molecular mechanics:

This method is based on the classical Hooke's law or harmonic oscillator, which treats the chemical bond between two adjacent atoms as a spring with a force constant k. The restoring force (F) between these two atoms is proportional to the displacement from the rest position(x) as seen in Eq. 2.

$$F = -kx \qquad \text{Eq. 1}$$

The potential energy (U) of the spring is:

$$U = 1/2\ kx^2 \qquad \text{Eq. 2}$$

This method tries to reproduce experimental data using parameterization of mechanical and electronic interactions. The potential energy of the molecule is the summation of stretching, bending, torsional motions and van der Waals interactions over the molecule in addition to charge-charge and dipole-dipole effects.

## 2b) Hartree-Fock model [6]

Hartree-Fock (HF) or *ab initio* method approximates the true many-electron wave-function as a product of the number of single electron wavefunctions, in determinational form. The energy of the system is obtained using the variation method, which minimizes the energy with respect to the coefficients of the orbitals. It is based on the Born-Oppenheimer approximation, which states that nuclear motion is independent of electronic

motion. Furthermore, it states that the nuclei are frozen in their equilibrium position on the time scale of the electronic motion. In the Hartree-Fock model, a Slater type orbital (S) is used, which has the following form:

$$S_{n,l,m}=N_{(n,l)}\, r^{n-1}\, e^{-\zeta r}\, Y_m(\theta,\varphi) \qquad \text{Eq. 3}$$

Where $\zeta$ is the adjustable parameter and $Y_m(\theta,\varphi)$ are the spherical harmonics. This function is approximated using a linear combination of one to six Gaussian type orbitals according to the following equation:

$$\Phi(r) = (2\alpha/\pi)^{3/4}\, e^{-\alpha r^{**}2} \qquad \text{Eq. 4}$$

The HF approximation which states that the many–electron wavefunction can be approximated using a multiplication after one-electron-functions follows, from the assumption that the electron solutions for the many-electron molecule will closely resemble a combination of one-electronic energy solutions for the hydrogen atom. Various levels of HF theory are possible, and some selection is required depending on the system to be investigated, the accuracy desired, and the computer resources at hand.

## 2b 1) Closed-shell determinantal wavefunctions [6]

Closed shell (means no unpaired electrons), single determinant wave functions characterize the most commonly used form of HF theory, and they are appropriate for the description of the ground states of most molecules with an even number of electrons.

## 2b 2) STO-3G minimal basis set [6]

The basis set termed STO-3G consists of minimal basis, and it uses Slater type orbitals and expands each one in terms of three Gaussian functions. This is important because it approximates the Slater type functions in terms of three mathematically manageable Gaussian functions. Slater type orbitals are mathematically difficult, and their calculations are time consuming to perform because of the evaluation of two electron integrals. Gaussian functions can be evaluated analytically due to the exponential ($-r^2$) term, which is not available in Slater type orbitals (which depend on exp (-r)).

## 2b 3) 6-21G and 3-21G split valence basis sets: [7]

These basis sets are representations in which each outer shell orbital (except for H) is represented by two functions, one contracted and the other diffuse. In each case, the inner functions are composed of two Gaussians while the outer (diffuse) functions are made up of only one Gaussian. In the 6-21G basis set, each inner-shell atomic orbital ((1s) for second row atoms) is written in terms of six Gaussian primitives.

## 2b 4) 6-31G* basis set: [7]

This basis uses six Gaussian primitives for the core orbitals, and a three/one split pair for each s-and p-valence orbital and a single set of six-d-functions, second order Gaussians which are equivalent to one s and five d-orbitals.

.

## 2b 5) 6-31G** basis set: [7]

This basis set has in addition to 6-31G*, a set of p-orbitals which has been added to each hydrogen to allow for polarization in hydrogen bonding. The p-orbitals perform the same function for the s-valence orbital of hydrogen, as the d-orbitals do for the p-valence orbitals in the second row elements.

## 2b 6) 6-311G basis set: [7]

A higher level of valence shell splitting is contained in the 6-311G basis set. As before, the inner-shell atomic orbitals are represented in terms of six Gaussian primitives, but it splits the valence functions into three parts instead of two, these being written in terms of three, one and one Gaussian primitives, respectively.

## 2c) Density Functional Theory: [6]

Density Functional Theory (DFT) is a technique for solving the Schroedinger equation:

$$H\psi=E\psi \qquad \text{Eq. 5}$$

Where the Hamiltonian operator H is a combination of kinetic and potential energy operators, which account for the interacting electrons, the nuclear-electron attraction, coulombic repulsion of the nuclei and a final term for the exchange and correlation energy of the electrons. DFT is an accurate method for predicting the ground state energy of the compounds. The idea behind DFT is to describe the interacting system of electrons by means of its charge density and not via many electron wavefunctions.

For the electron density, the basic variables of the system depend only on three coordinates x, y, and z rather than the 3N variables required for describing the N-electron wave function. The electron exchange correlation functionals (function of a function) are usually described as functions, which result from operating on the electronic density distribution[7]. The exchange correlation functional may be approximated using the following different techniques: Such as local density approximation (LDA), non local extension to LDA, and hybrid Functional Methods.

The LDA functional can be regarded as an exchange co-relational functional for a homogeneous electron gas. The first DFT model was put forward independently by L.H. Thomas and E. Fermi[8] before the introduction of Hartree-Fock theory. They simply

assumed the existence of energy functional and derived an expression for the kinetic energy based on the density of electrons, ρ (r), in an infinitive potential well. This kinetic energy functional is given by:

$$T_{TF}(\rho) = (3/10)\,(3\pi^2)^{2/3}\int dr\ \rho^{5/3}(r) \qquad \textbf{Eq. 6}$$

This equation is one of the most important ideas of modern physics, since it is the first introduction of a local density approximation. The Thomas-Fermi energy is given as a sum of electronic kinetic energy (T), and the electron nucleus attraction energy and the Hartree correlation energy.

In 1964 Hohenberg and Kohn[8] were working together in Paris investigating the foundation of the Thomas-Fermi model. They gave proofs of two important theorems. They considered that an electronic system with a given Hamiltonian has ground state energy as well as a ground state wavefunction, which is completely determined by the minimization of the total energy as a functional of the wavefunction. They also assumed that the external potential, together with the number of electrons, completely determines the Hamiltonian, and that these two quantities determine all the properties of the ground state.

The first Hohenberg-Kohn theorem[8] states: "The external potential v(r) is determined, within a trivial additive constant, by the electron density ρ(r). Since the electron density is determined by the number of electrons, it follows that the electron density determines the

wavefunction and thereby all of the ground state properties of the system. The proof of the theorem assumes the existence of two external potentials which differ by more than a constant, and which lead to the same ground state density. This implies the existence of two different Hamiltonians, with differing wavefunctions, corresponding to the same ground state electron density. The electron density determines all properties of the ground state including the total ground state energy, $E_{tot}$, the ground state kinetic energy, T, the energy of the electrons in the external potential, U, and the electron-electron interaction energies, W; all of these are functionals of the electron density. The total energy can therefore be written as:

$$\mathbf{E^0_{(tot)} = E_{tot}(\rho^0) = T(\rho^0) + U(\rho^0) + W(\rho^0)} \qquad \textbf{Eq. 7}$$

Where $\rho^0$ denotes the true ground state electron density of the system. The first Hohenberg-Kohn theorem, thus, establishes the existence of the total energy functional, but it does not provide the solution to many body electron problems.

The second Hohenberg-Kohn theorem provides a variational principle. "For any given non-negative trial density, $\rho(r)$, that integrates to the correct number of electrons, N, the true ground state energy $E^0_{(tot)}$ satisfies the relation".[8]

$$\mathbf{E^0_{(tot)} < E_{tot}(\rho(r))} \qquad \textbf{Eq. 8}$$

The exchange and correlation energy functional is not in general equivalent to the quantum chemical exchange and correlation. The inclusion of correlation effects in the KS

orbitals make these different from the HF-orbitals. If one would use the same orbitals in both methods, the same operator would be used for kinetic energy, and the external potential would also be the same. The total exchange and co-relational energy in the two descriptions would therefore be the same.

In this approximation, the canonical Kohn-Sham equations are obtained:

$$[- ½ (\partial^2/\partial\tau^2)_i + V_{eff}] \Psi_i = \varepsilon_i \psi_i \qquad \textbf{Eq. 9}$$

Where $\tau$ includes coordinate x, y, and z and i runs over all electrons, $c_i$ is the Kohn-Sham eigenvalue of electron, i, and the effective potential ($V_{eff}$) is seen in eq.10 $r^2 = x^2 + y^2 + z^2$

$$V_{eff}(r) = V_{ext}(r) + \int dr' \rho(r')/(r - r') + V_{xc}(r) \qquad \textbf{Eq. 10}$$

$V_{ext}$ is the external potential and the exchange-correlation potential ($V_{xc}$) is defined as the functional derivative of the exchange and correlation energy ($E_{xc}$) with respect to the electron density:

$$V_{xc}(r) = \partial E_{xc}[\rho(r)] / \partial \rho(r) \qquad \textbf{Eq. 11}$$

These equations are non-linear like the Hartree-Fock equations and are thus solved by an equivalent self-consistent (iterative) procedure. The resulting density is described below:

$$\rho(r) = \Sigma_I \Psi_i^*(r)\, \Psi_i(r) \qquad \text{Eq. 12}$$

The Kohn-Sham eigenvalues, then, give the total ground state energy using either of two equivalent solutions:

$$E_{tot}(\rho) = T_s(\rho) + U(\rho) + H(\rho) + E_{xc}(\rho) \qquad \text{Eq. 13}$$

Or:

$$E_{tot}(\rho) = \Sigma_I(\varepsilon_i) - \tfrac{1}{2} \int drdr' \, \rho(r)\, \rho(r')/(r - r') + E_{xc}(\rho) - \int dr V_{xc}(r)\, \rho(r) \qquad \text{Eq. 14}$$

The non-local extension to **LDA** is necessary because molecules are realistically in a heterogeneous electron gas, not a homogeneous one. A hybrid functional employs Hartree-Fock treatment for the exchange term as repulsion integrals. **B3LYP** is a particular density functional method due to Lee, Yang and Parr, and **B3** signifies a 3 parameter functional due to Axel Becke.[7]

## 2d) Semi-empirical methods[6]

These methods follow directly from Hartree-Fock models, and are based on the simplification that valence electrons are the only ones to be considered in the calculations. The inner electrons are regarded as a part of a fixed core. The central approximation in the semi-empirical methods is to assume that atomic orbitals residing on different atoms do not overlap. The semi-empirical method relies on parameterization of atomic orbital interactions, and these adjustable parameters are chosen to reproduce equilibrium geometries, enthalpies of formation, ionization potentials and dipole moments. The **AM1**[9] and **PM3**[9] models use the same approximations for differential overlap, but differ in their in their parameterization. **AM1** and **PM3** are extensions to the **MNDO** method which signifies Modified Neglect of Diatomic Overlap. Diatomic overlap refers to interaction of atomic orbitals on different atomic centers.

The earlier **AM1** is parameterized for H, C, N and O atoms exclusively, the so called organic elements. **PM3** stands for parameterized model 3, and it has advantage over **AM1** in that it is parameterized for more atoms (i.e., 3rd nonmetals plus aluminium and halogens). It, thus, allows a wider range of molecules in the computations. **AM1** and **PM3** are parameterized to yield the energies of molecules in the form of standard enthalpies of formation (where the enthalpies of the elements are set to zero at 298 K and 1 bar). This stands in contrast to the Hartree-Fock model, which yields total energy $E_{tot}$ at 0K (where the zero-energy state is a frozen nuclear framework and the separated electrons). **AM1** was developed because the **MNDO** method failed to reproduce steric interference and

hydrogen bonding. Energy effects were too positive for crowded molecules such as neopentane, and were too negative for molecules containing four-membered rings. Activation energies also tended to be too large. A common cause for the errors in **MNDO** is the tendency to overestimate repulsions between neighbouring atoms. **AM1** deals with this repulsion by adding additional gaussian functions, in the form of a core repulsion function (CRF), for any pair of atoms **AB** in the molecule.

$$\mathbf{CRF\ (AB) = [zAzB\ \gamma_{ss}]\ [1 + F\ (A) + F\ (B)]} \qquad \textbf{Eq. 15}$$

$$\mathbf{F\ (A) = \exp\ (-\ \alpha_A\ R_{AB}) + \Sigma_I K_{Ai} \exp[L_{Ai}(R_{AB} - M_{Ai})^2]} \qquad \textbf{Eq. 16}$$

$$\mathbf{F\ (B) = \exp\ (-\alpha_B R_{AB}) + \Sigma_j\ K_{Bj} \exp[L_{Bj}\ (R_{AB} - M_{Bj})^2]} \qquad \textbf{Eq. 17}$$

Where α, L, K and M are further adjustable parameters. Two ways were used to reduce the excessive interatomic repulsions at large separation. In the first reduction, one or more attractive gaussians were added to compensate directly. In the second reduction, repulsive gaussian functions were centered at smaller internuclear separations

The **MNDO** method which is the basis for **AM1** and **PM3** methods is itself based on the Hartree-Fock method. The treatment with **MNDO** is confined to the valence electrons of closed shell molecules. These electrons are assumed to move in the field of the fixed core potentials of the nuclei and of the inner shell electrons (core repulsion). The valence shell AO's, $\Phi_v$

$$\Psi_i = \Sigma_\nu C_{\nu i} \Phi_\nu \qquad \text{Eq. 18}$$

The coefficients $C_{\nu i}$ are found from the Roothan-Hall equations (the variation method) which assume the form:

$$\Sigma_\nu (F_{\mu\nu} - E_i \delta_{\mu\nu}) = 0 \qquad \text{Eq. 19}$$

Where $E_i$ is the eigenvalue of the **MO** $\psi_i$ and $\delta_{\mu\nu}$ is the Kronecker $\delta$. The elements $F_{\mu\nu}$ of the Fock matrix are the sum of a one electron part $\mathbf{H}_{\mu\nu}$ (core Hamiltonian), and a two electron part $\mathbf{G}_{\mu\nu}$;

$$F_{\mu\nu} = H_{\mu\nu} + G_{\mu\nu} \qquad \text{Eq. 20}$$

The electronic energy $E_{el}$ is given by eq.21 Where $\rho_{\mu\nu}$ is an element of the bond order matrix.

$$E_{el} = \tfrac{1}{2} \Sigma_\mu \Sigma_\nu P_{\mu\nu} (H_{\mu\nu} + F_{\mu\nu}) \qquad \text{Eq. 21}$$

It is assumed that AO's $\Phi_\mu$ and $\Phi_\nu$ are centered at atom A and the AO's $\Phi_\lambda$ and $\Phi_\sigma$ are at atom B (A≠B). The Fock matrix elements then are:

$$F_{\mu\mu} = U_{\mu\mu} \Sigma_B V_{\mu\mu, B} + \Sigma_{\nu, A} P_{\nu\nu}[(\mu\mu, \nu\nu) - \tfrac{1}{2} (\mu\nu, \mu\nu)] + \Sigma_B \Sigma_{\lambda, \sigma} P_{\lambda\sigma}(\mu\mu,\lambda\sigma) \qquad \text{Eq. 22}$$

$$F_{\mu\nu} = \Sigma_B V_{\mu\nu,\,B} + \tfrac{1}{2} P_{\mu\nu} [3(\mu\nu,\mu\nu) - (\mu\mu,\nu\nu)] + \Sigma_B \Sigma_{\lambda\sigma} (\mu\nu,\lambda\sigma) \qquad \textbf{Eq. 23}$$

$$F_{\mu\lambda} = \beta_{\mu\lambda} - \tfrac{1}{2} \Sigma_{\nu,\,A} \Sigma\sigma_{,\,B} P_{\nu\sigma} (\mu\nu, \lambda\sigma) \qquad \textbf{Eq. 24}$$

The Fock matrix has the following six terms:

1) One-center one-electron energies $U_{\mu\nu}$ which represent the sum of the kinetic energy of an electron in AO $\Phi_\mu$ at atom A and its potential energy due to the attraction of the core of atom. $U_{\mu\nu}$ assumes the following form:

$$U_{\mu\nu} = (\partial^2\Phi_\mu/\partial\tau_1) - (e^2/r_1)\,\Phi_\mu d\tau \qquad \textbf{Eq. 25}$$

2) One-center two-electron repulsion integrals, i.e., Coulomb integrals.

$$(\mu\mu, \nu\nu) = g_{\mu\nu} \qquad \textbf{Eq. 26}$$

3) Exchange integrals

$$(\mu\nu, \mu\nu) = h_{\mu\nu} \qquad \textbf{Eq. 27}$$

4) Two-center one-electron core resonance integrals $\beta_{\mu\lambda}$

$$\beta_{\mu\lambda} = \int\Phi_\mu\,(e^2/r_B)\,\Phi_\lambda\,d\tau_\lambda \qquad \textbf{Eq. 28}$$

5) Two center one-electron attractions $V_{\mu\nu, B}$ between an electron in the distribution $\Psi_\mu\Psi_\nu$ at atom A and the core of atom B.

6) Two-center two-electron repulsion integrals ($\mu\nu$, $\lambda\sigma$). These integrals represent the energy of interaction between the charge distribution at atom A and atom B, and they have the following form:

$$(\mu\nu, \lambda\sigma) = \iint \Phi_\mu^{*(1)} \Phi\nu^{(1)} [1/r_{12}] \Phi\lambda^{*(2)} \Phi_\sigma^{(2)} d\tau_1 d\tau_2 \qquad \textbf{Eq. 29}$$

The total energy of the molecule $E_{tot}$ is the sum of the electronic energy $E_{el}$ and the repulsions between the cores of atoms A and B ($E_{AB}^{core}$).

$$E_{tot}^{mol} = E_{el} + \Sigma_A \Sigma_B E_{AB}^{core} \qquad \textbf{Eq. 30}$$

The heat of formation of the molecule is obtained from its total by subtracting the electronic energies and adding the experimental heats of formation of the atoms ($\Delta H_f$) in the molecule:

$$\Delta H_f^{mol} = E_{tot}^{mol} - \Sigma_A E_{el}^{A} + \Sigma_A \Delta H_f^{A} \qquad \textbf{Eq. 31}$$

The electronic energies of the atoms are calculated from restricted single-determinantal wavefunctions using the same approximations and parameters as in molecular **MNDO** calculations.

## 2e) Thermodynamics and Kinetics:

A wide variety of thermodynamic properties can be calculated from computer simulations, and comparison of experimental and calculated values for such properties is an important way in which the accuracy of the simulation and the underlying energy model can be quantified. Simulation methods also enable predictions to be made of the thermodynamic properties of systems for which there is no experimental data, or for which experimental data is difficult or impossible to obtain. Simulations can also provide structural information about the conformational changes in molecules and the distributions of molecules in a system. Unfortunately, the free energy is a difficult quantity to obtain in systems such as liquids or flexible macromolecules that have many minimum energy configurations separated by low-energy barriers and intermolecular interactions. Associated quantities such as entropy and chemical potential are also difficult to calculate in such condensed phases.

The equilibrium constant for the reaction is a thermodynamic property of the reactants and products and is a function of the standard Gibb's free energy, $\Delta G^0$, according to the following equation:

$$\Delta G^0 = -RT\ln K_c \qquad \textbf{Eq. 32}$$

Where R is the gas constant and T is the absolute temperature and $K_e$ is the equilibrium constant.

In general,

$\Delta G^0 > 0$ refers to a nonspontaneous reaction;

$\Delta G^0 = 0$ refers to an equilibrium state of the reaction;

$\Delta G^0 < 0$ refers to a spontaneous reaction;

$\Delta G^0$ is related to the standard entropy and enthalpy of the reaction by the following equation. The superscript ( $^0$ ) refers to the standard conditions at 298K and 1 bar pressure.

$$\Delta G^0 = \Delta H^0 - T\,\Delta S^0 \qquad \textbf{Eq. 33}$$

Our calculations give $\Delta H^0$ and $\Delta S^0$ for individual compounds, from which we calculate $\Delta G^0$.

The rate constant of a reaction is a kinetic property and is related to the activation energy by the Arrhenius equation;

$$\ln k_l = \ln A - E_a/RT \qquad \textbf{Eq. 34}$$

where $k_l$ is the rate constant and A is a frequency factor. The alternative Eyring equation gives a relation which links the rate constant and the equilibrium constant between the reactants and transition state;

$$k_l = (kT/h)\,K^{\dagger} \qquad \textbf{Eq. 35}$$

where k is the Boltzmann constant, h is the Planck constant and $K^{\dagger}$ is the equilibrium constant between reactants and transition state. The superscript (†) refers to this

equilibrium. The free energy of activation is related to the enthalpy of activation and entropy of activation by the equation given below:

$$\Delta G^{\dagger} = \Delta H^{\dagger} - T\,\Delta S^{\dagger} \qquad \textbf{Eq. 36}$$

The activation energy $E_a$ is related to the enthalpy of activation $\Delta H^{\dagger}$ by the following equation;

$$E_a = \Delta H^{\dagger} + 2RT \qquad \textbf{Eq. 37}$$

## 2f) Modeling chemical reactions and electron correlation effects:[8]

The preferred technique for modeling chemical reactions is usually considered to be quantum mechanics, but if one wishes to represent the whole system explicitly, the large number atoms that must be considered is rarely practical in the case of *ab initio* quantum mechanics. Furthermore, environmental effects such as solvent interactions are not readily taken into account. We consider three methods used to study chemical reactions that involve large molecules. One strategy is to use a purely empirical approach. An alternative is to divide the system into two parts and treat the reaction region using quantum mechanics, and the rest of the system being modeled using molecular mechanics. Third, is to use techniques such as density functional theory or Carloni-Parrinello method.

The empirical approaches employ force field models for studying reactions, which are used to estimate the activation energies of possible transition states to explain the reaction. The force field model is usually derived by extending an existing force field to enable the

structures and relative energies of transition structures to be determined. This second approach to simulate chemical reactions in solution is to use a combination of quantum mechanics and molecular mechanics. The reacting parts of the system are treated quantum mechanically, with the remainder being modeled using the force field. The total energy $E_{TOT}$ for a system can be written as

$$E_{TOT} = E_{QM} + E_{MM} + E_{QM/EM} \qquad \textbf{Eq. 38}$$

where $E_{QM}$ is the energy of those parts of the system treated exclusively with quantum mechanics, and $E_{MM}$ is the energy of the purely molecular mechanical parts of the system. $E_{QM\,MM}$ is entirely due to non-bonded interactions between the quantum mechanical and molecular mechanical parts of the system.

It is well known that ignoring electron correlation and bond harmonicities contribute an error of 10% of the energy of a typical calculation. Moller-Plesset theory (MP2, MP3 etc.) provides a way to correct for the electron correlation error by including electronically excited state configurations in the ground state wavefunction.

## 2g) Effect of solvation:

Since nearly all computer models are based on gas phase molecules or ions, their results may be influenced by solvent effects. They are impractical to include in a specific way, but may be crudely reflected in molecular mechanics calculations. Generally the effects are small when considering entropy and geometry changes, but may become significant in process involving changes in polarity.

# CHAPTER 3

## Results and Discussion

### Introduction:

This project is done at several theoretical levels to calculate thermodynamic and kinetic properties using semi-empirical, density functional theory and electron correlation methods. Strains of antibiotic resistant bacteria have arisen owing to their possession of β- lactamases that catalyze the hydrolysis of the fused four member ring of β- lactams found in Penicillin and Cephalosporin drugs.

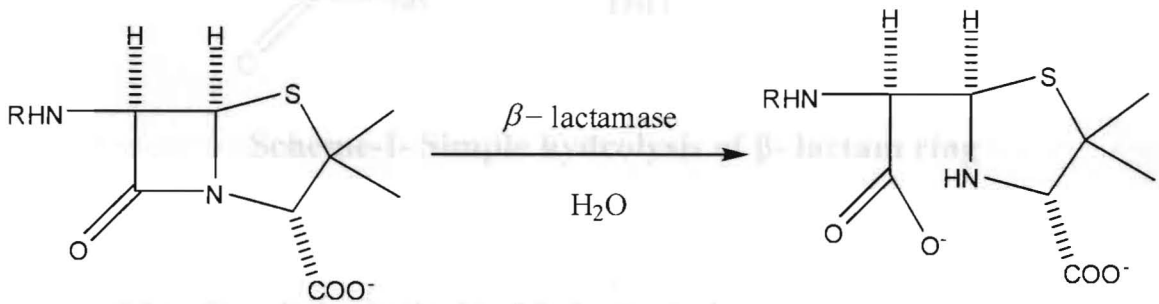


**General hydrolysis reaction of Penicillins**

The resulting monocyclic molecule no longer inhibits a transpeptidase that is necessary for bacterial cell wall synthesis. Molecular modeling of the transition state of class B-β-lactamases has given insight to how hydrolyzing the C-N bond of the β- lactam ring hydrolyzes and the role of zinc ions.

## A) Thermodynamics:

The heat of formation and entropies (translational, rotational and vibrational) were calculated for each reactant and product by the standard statistical thermodynamic methods. $\Delta H_{Rxn}$, $\Delta S_{Rxn}$, and $\Delta G_{Rxn}$ for the reaction at semi-empirical (AM1 and PM3), Hartree-Fock and density functional theory (B3LYP at 6-31G*) and MP2 (β- lactam ring) levels of treatment, but for benzyl Penicillin only on semi-empirical (AM1 and PM3) levels of treatments.

### A1) Results

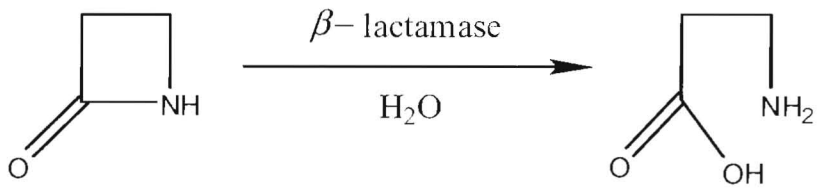


**Scheme-I- Simple hydrolysis of β- lactam ring**

### A1a) Simple hydrolysis of β- lactam ring

Table- 1 shows computed values of heats of formation of the reactants (β-lactam and water) and product (hydrolyzed β- lactam ring). For the heats of formation of the model reaction compounds are in table- 1.

**Figure 5:** Optimized structure at B3LYP/6-31G* of β- lactam ring at the initial state (reactant).

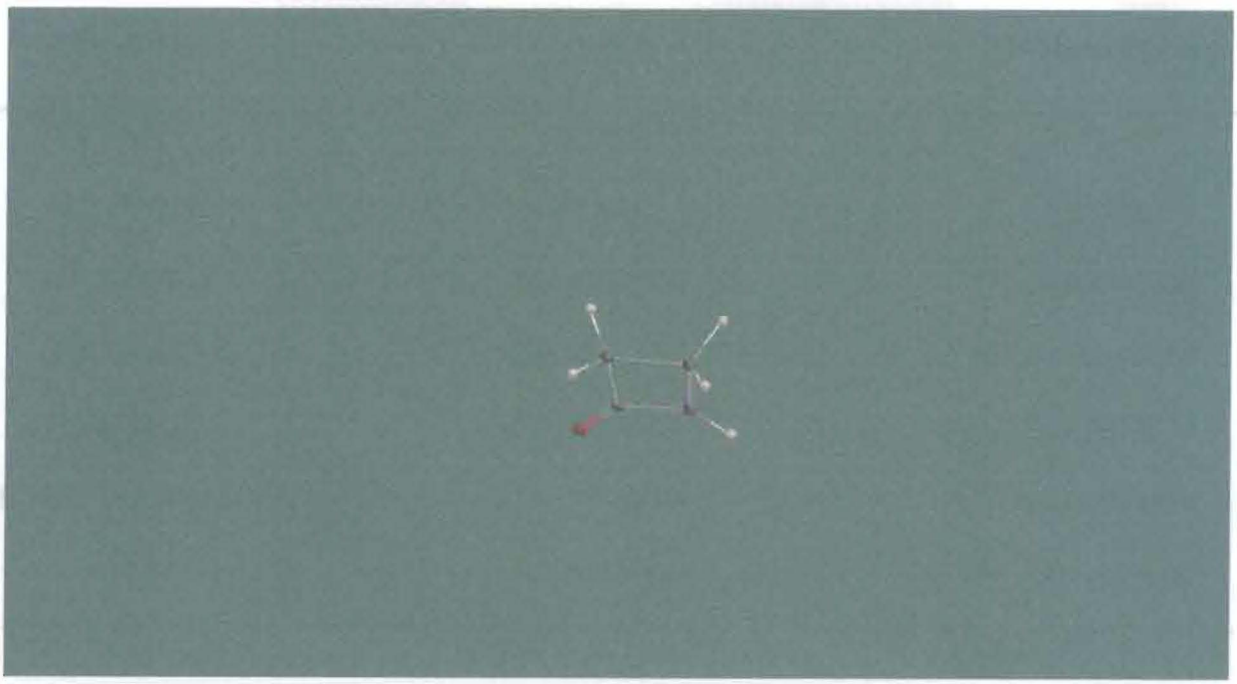

**Figure 6:** Optimized structure at B3LYP/6-31G* of β- lactam at the final state (product).

**Table-1**: Heat of formation of β- lactam ring hydrolysis reaction components.

| LEVEL OF THEORY | Units | β- lactam ring | Water | Hydrolyzed β- lactam ring |
|---|---|---|---|---|
| SE (AM1) | (kcal/mol) | -21.849 | -59.240 | -106.468 |
| SE (PM3) | (kcal/mol) | -21.849 | -53.240 | -99.5347 |
| HF 3-21G(*) | au | -244.4329365 | -75.5859597 | -320.0701748 |
| HF 6-31G* | au | -245.8104325 | -76.0107465 | -321.8675088 |
| HF 6-31G** | au | -245.8209986 | -76.236150 | -321.8876274 |
| DF-B3LYP 6-31G* | au | -247.2856180 | -76.4089462 | -321.7384904 |
| MP2 | au | -246.5277514 | -76.1968476 | -322.768428 |

Table- 2 shows computed values of entropies (translation, rotational, and vibrational) of reactants and products. Electronic degeneracies are included in modeling programs, but open shell systems are still difficult to predict accurately.

**Table-2**: Absolute entropy of β- lactam ring hydrolysis reaction components (J/mol.K).

| LEVEL OF THEORY | β- lactam ring | Water | Hydrolyzed β- lactam ring |
|---|---|---|---|
| SE (AM1) | 284.25 | 188.65 | 337.16 |
| SE (PM3) | 284.25 | 188.24 | 343.06 |
| HF 3-21G(*) | 285.11 | 188.64 | 331.10 |
| HF 6-31G* | 293.21 | 188.22 | 331.60 |
| HF 6-31G** | 291.10 | 188.10 | 331.82 |
| DF-B3LYP 6-31G* | 293.40 | 188.85 | 336.90 |
| MP2 | 303.47 | 172.97 | 334.58 |

**Table-3**: $\Delta H_{Rxn}$, $\Delta S_{Rxn}$ and $\Delta G_{Rxn}$ of β- lactam ring hydrolysis reaction.

| LEVEL OF THEORY | $\Delta H_{Rxn}$ kcal/mol | $\Delta S_{Rxn}$ cal/Kmol | $\Delta G_{Rxn}$ kcal/mol |
|---|---|---|---|
| SE (AM1) | -25.551 | -0.0324 | -15.90 |
| SE (PM3) | -24.259 | -0.03092 | -15.11 |
| HF 3-21G(*) | -29.29 | -0.02762 | -21.06 |
| HF 6-31G* | -28.47 | -0.03580 | -17.67 |
| HF 6-31G** | -26.40 | -0.03590 | -15.71 |
| DF-B3LYP 6-31G* | -26.96 | -0.03427 | -16.84 |
| MP2 | -64.32 | -0.03389 | -54.22 |

Table- 3 shows $\Delta H_{Rxn}$, $\Delta S_{Rxn}$ and $\Delta G_{Rxn}$ of β- lactam ring hydrolysis reaction at defferent levels of theories.

## A1b) fused β- lactam and thiol ring

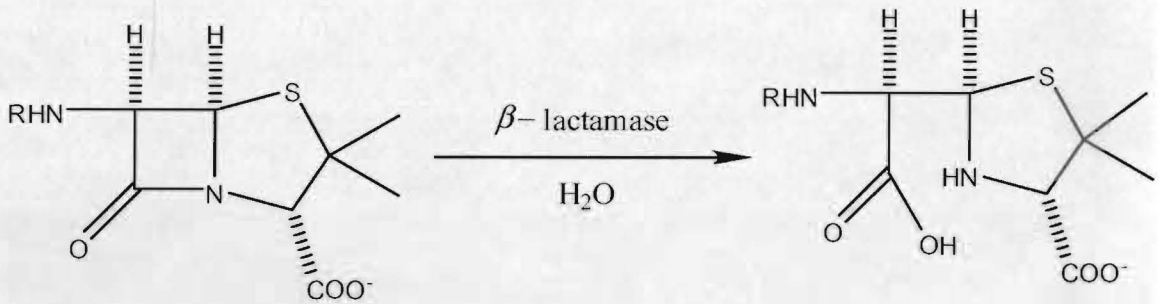


**Scheme-II- Hydrolysis of fused β- lactam and thiol ring**

Table- 4 shows computed values of heats of formation of the reactants (fused β- lactam thiol ring and water) and product (hydrolyzed fused β- lactam thiol ring). For the heats of formation of the model reaction compounds are in table- 4.

**Figure 7:** Optimized structure at B3LYP/6-31G* of fused β- lactam thiol ring at the initial state (reactant).

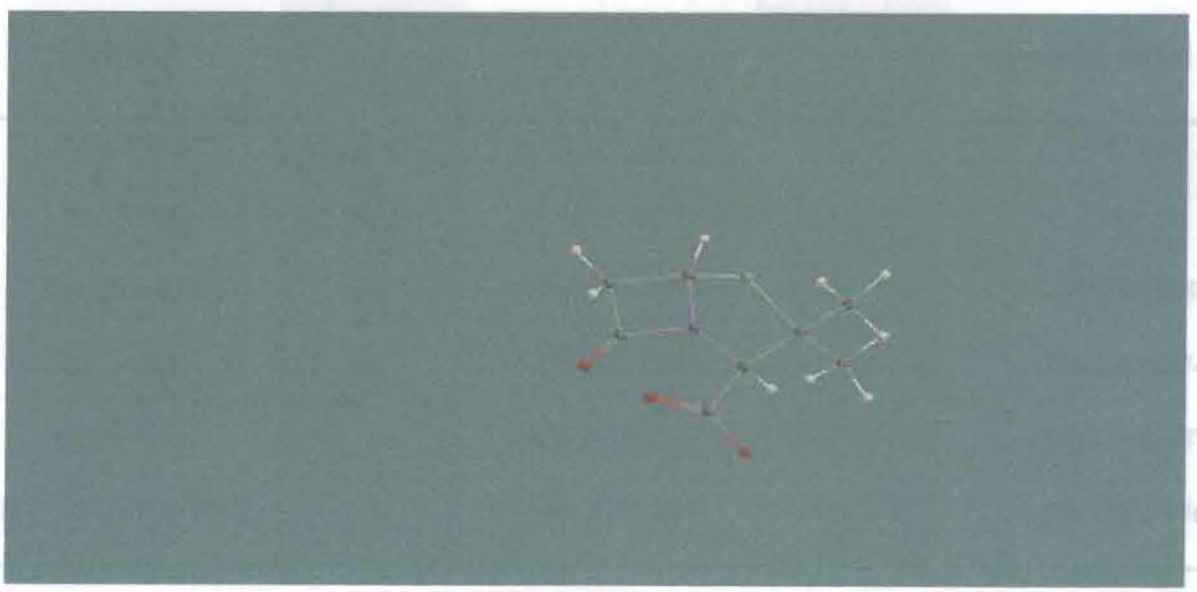

**Figure 8:** Optimized structure at B3LYP/6-31G* of fused β- lactam thiol ring at the final state (product).

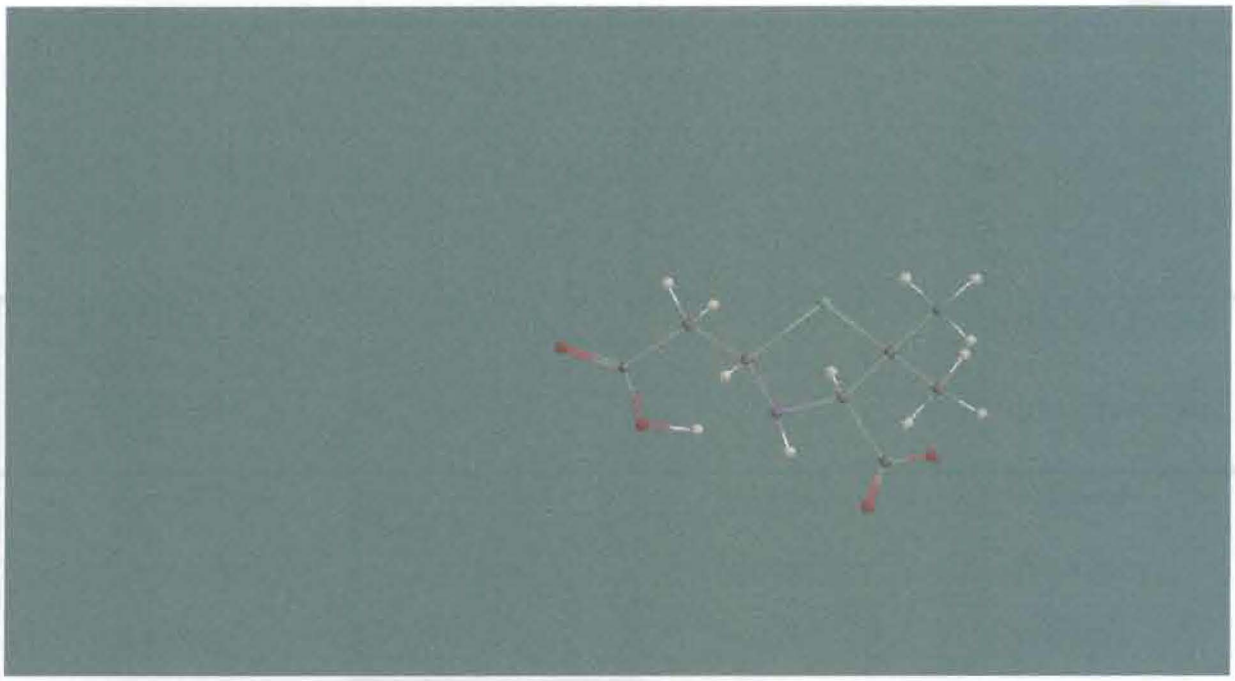

**Table-4**: Heat of formation of fused β- lactam thiol ring hydrolysis reaction components.

| LEVEL OF THEORY | Units | Fused β- lactam thiol ring | Water | Hydrolyzed fused β- lactam thiol ring |
|---|---|---|---|---|
| SE (AM1) | (kcal/mol) | -110.341 | -59.240 | -217.647 |
| SE (PM3) | (kcal/mol) | -133.00 | 53.240 | 218.197 |
| HF 3-21G(*) | au | -980.1174750 | -75.585997 | -1055868753 |
| HF 6-31G* | au | -985.3350454 | -76.0107465 | -1061.4168746 |
| HF 6-31G** | au | -985.3506188 | -76.0236150 | -1061.4426871 |
| DF-B3LYP 6-31G* | au | -989.5213899 | -76.4089462 | -1066.0061766 |

Table- 5 shows computed values of entropies (translation, rotational, and vibrational) of reactants and products. Electronic degeneracies are included in modeling programs, but open shell systems are still difficult to predict accurately.

**Table-5**: Absolute entropy of fused β-lactam thiol ring hydrolysis reaction components (J/mol.K).

| LEVEL OF THEORY | Fused β- lactam thiol ring | Water | Hydrolyzed fused β- lactam thiol ring |
|---|---|---|---|
| SE (AM1) | 453.9411 | 188.6524 | 498.5466 |
| SE (PM3) | 451.8609 | 188.2397 | 495.4969 |
| HF 3-21G(*) | 474.1151 | 188.6476 | 474.1413 |
| HF 6-31G* | 435.2716 | 188.2281 | 479.9653 |
| HF 6-31G** | 435.8803 | 188.0984 | 480.7982 |
| DF-B3LYP 6-31G* | 449.9872 | 188.6476 | 493.5378 |

**Table-6**: $\Delta H_{Rxn}$, $\Delta S_{Rxn}$ and $\Delta G_{Rxn}$ of fused β- lactam thiol ring hydrolysis reaction.

| LEVEL OF THEORY | $\Delta H_{Rxn}$ kcal/mol | $\Delta S_{Rxn}$ cal/Kmol | $\Delta G_{Rxn}$ kcal/mol |
|---|---|---|---|
| SE (AM1) | -48.066 | -0.03441 | -38.41 |
| SE (PM3) | -31.357 | -0.03456 | -22.14 |
| HF 3-21G(*) | -102.58 | -0.04500 | -94.35 |
| HF 6-31G* | -44.00 | -0.03430 | -33.33 |
| HF 6-31G** | -42.95 | -0.03430 | -32.83 |
| DF-B3LYP 6-31G* | -46.98 | -0.03460 | -36.88 |

Table- 6 shows $\Delta H_{Rxn}$, $\Delta S_{Rxn}$ and $\Delta G_{Rxn}$ of fused β- lactam thiol ring hydrolysis reaction at defferen level of theories.

## A1c) Benzyl Penicillin

Table- 7 shows computed values of heats of formation of the reactants (benzyl Penicillin and water) and product (hydrolyzed benzyl Penicillin). For the heats of formation of the model reaction compounds are in table- 7.

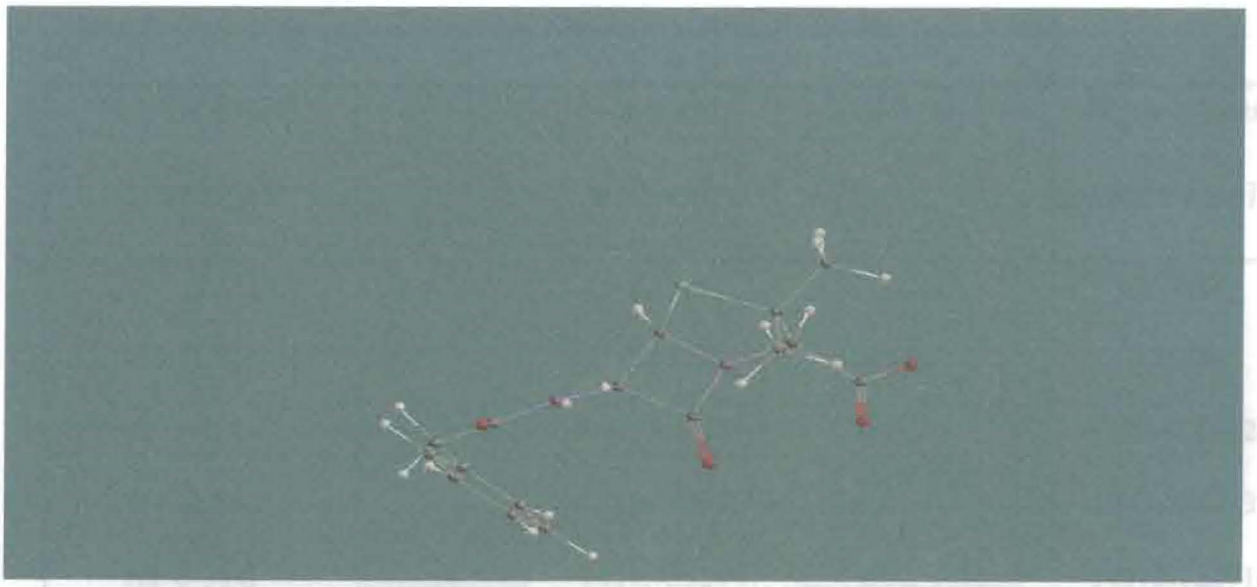

**Figure 9:** Optimized structure at B3LYP/6-31G* of benzyl Penicillin at the initial state (reactant).

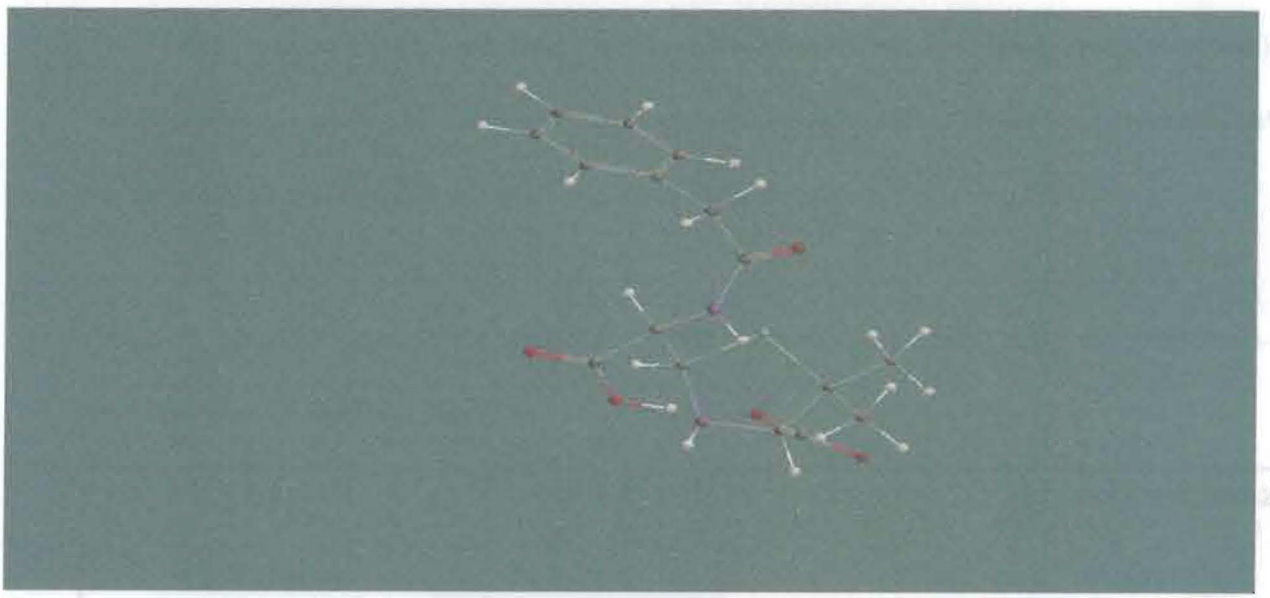

**Figure 10:** Optimized structure at B3LYP/6-31G* of benzyl Penicillin at the final state (product).

**Table-7**: Heat of formation of benzyl Penicillin hydrolysis reaction components.

| LEVEL OF THEORY | Units | Benzyl Penicillin | Water | Hydrolyzed benzyl Penicillin |
|---|---|---|---|---|
| SE (AM1) | (kcal/mol) | -121.34 | -59.240 | -223.92 |
| SE (PM3) | (kcal/mol) | -144.35 | 53.240 | 231.70 |
| HF 3-21G(*) | au | -1414.1255871 | -75.585997 | -1489.8010224 |
| HF 6-31G* | au | -1421.6999999 | -76.0107465 | -1497.7717631 |
| HF 6-31G** | au | -1421.7302047 | -76.0236150 | -1497.8122914 |
| DF-B3LYP 6-31G* | au | -1428.5964000 | -76.4089462 | -1505.0650973 |

Table- 8 shows computed values of entropies (translation, rotational, and vibrational) of reactants and products. Electronic degeneracies are included in modeling programs, but open shell systems are still difficult to predict accurately.

**Table-8**: Absolute entropy of benzyl Penicillin hydrolysis reaction components at semi-empirical level of theory (J/mol.K).

| LEVEL OF THEORY | Benzyl Penicillin | Water | Hydrolyzed benzyl Penicillin |
|---|---|---|---|
| SE (AM1) | 655.2819 | 188.6524 | 660.1519 |
| SE (PM3) | 667.7385 | 188.2386 | 661.1569 |

**Table-9**: $\Delta H_{Rxn}$, $\Delta S_{Rxn}$ and $\Delta G_{Rxn}$ of benzyl Penicillin hydrolysis reaction at semi-empirical level of theory.

| LEVEL OF THEORY | $\Delta H_{Rxn}$ kcal/mol | $\Delta S_{Rxn}$ cal/Kmol | $\Delta G_{Rxn}$ kcal/mol |
|---|---|---|---|
| SE (AM1) | -43.34 | -0.0439 | -30.25 |
| SE (PM3) | -33.93 | -0.0465 | -20.07 |

Table- 9 shows $\Delta H_{Rxn}$, $\Delta S_{Rxn}$ and $\Delta G_{Rxn}$ of benzyl Penicillin hydrolysis reaction at semi-empirical level of theory there is a gain in $\Delta H_{Rxn}$, and $\Delta S_{Rxn}$.

## A2) Discussion:

When we take up this reaction we want to see whether we can explain the kinetics and active site in a reasonable manner. For this we first started with the basic thermodynamic properties. A wide variety of thermodynamic properties can be calculated from computer simulations and calculated values for such properties are an important way in which the accuracy of the simulation and the underlying energy can be understood. Simulation method also enables predictions to be made on the thermodynamic properties of systems for which there is no experimental data or for which experimental data is difficult or impossible to obtain. As the molecules in the

present reaction are so complex it is not easy to calculate the higher level of theories such like Hartree-Fock and density functional theory.

## B) Building and locating transition state:

We used Spartan Pro™, 2004™ for building and locating transition states. The software assists in providing both an extensive and extendable library of calculated transition states and a facility for matching as closely as possible entries in the library with the reaction in hand. As the reaction is known to library a fallback technique similar to the linear synchronous transit method is automatically invoked which guesses the average of reactant and product geometries.

**Table-10:** Determination of the exact transition state in Lactam ring.

| BOND LENGTH | Set 1 | Set 2 | Set 3 | Set 4 | Set 5 | Set 6 | Set 7 | Set 8 | Set 9 | Set 10 | Set 11 | Set 12 |
|---|---|---|---|---|---|---|---|---|---|---|---|---|
| C-O Å | 2.2 | 2.1098 | 2.0196 | 1.9294 | 1.8392 | 1.519 | 1.749 | 1.6702 | 1.5914 | 1.5126 | 1.4338 | 1.355 |
| N-H Å | 2.2 | 1.9982 | 1.7964 | 1.5946 | 1.3928 | 1.36 | 1.191 | 1.1526 | 1.1142 | 1.0758 | 1.0374 | 0.999 |
| C-N Å | 1.352 | 1.4072 | 1.4624 | 1.5176 | 1.5728 | 1.69 | 1.628 | 1.9306 | 2.2332 | 2.5358 | 2.8384 | 3.141 |
| O-H Å | 0.951 | 1.0492 | 1.1474 | 1.2456 | 1.3438 | 1.244 | 1.442 | 1.6276 | 1.8132 | 1.9988 | 2.1844 | 2.37 |
| Min.Energy (kcal/mol) | 354.31 | 189.05 | 97.78 | 72.78 | 43.37 | 32.01 | 34.67 | 12.13 | 11.46 | 26.59 | 63.59 | 131.94 |
| Heat of formation (kcal/mol) | -6.36 | -30.45 | -35.65 | -57.47 | -69.47 | -28.9 | -51.3 | -37.01 | -47.15 | -57.05 | -66.05 | 69.32 |

Table- 10 shows the different bond length of C-O, N-H, C-N, and O-H in different sets to locate the exact transition state in lactam ring. Set 6 gave the minimum energy value and minimum heat of formation. So we took these bond lengths while building the transition state.

**Figure 11:** Optimized structure at B3LYP/6-31G* of β- lactam ring with water at the transition state.

## B1)Results:

### B1a) Transition state of β- lactam ring with water

**Table-11:** Shows computed values of ΔH of formation of reactants (water and β- lactam ring) and transition state at different levels (with no $Zn^{2+}$).

| LEVEL OF THEORY | Units | ΔH of reactants | ΔH of transition state |
|---|---|---|---|
| SE (AM1) | (kcal/mol) | -81.089 | 62.514 |
| SE (PM3) | (kcal/mol) | -75.089 | 62.800 |
| HF 3-21G(*) | au | -320.0188962 | -319.7864002 |
| HF 6-31G* | au | -321.8211790 | -321.5384724 |
| HF 6-31G** | au | -321.8446136 | -321.6669039 |
| DF-B3LYP 6-31G* | au | -323.6945642 | -323.5549224 |
| MP2 | au | -322.7245990 | -322.585239 |

Table- 12 shows activation energies at different levels of theory with no $Zn^{2+}$ present. Semi-empirical method gave the high value of $\Delta H^{\ddagger}$, and the activation energy steadily lowers as more functions are added to the HF basis set, DF-B3LYP at 6-31G* basis and MP2 basis set.

**Table-12:** Activation energy of β- lactam ring hydrolysis reaction without zinc at various levels of theory.

| LEVEL OF THEORY | Units | Activation energy |
|---|---|---|
| SE (AM1) | (kcal/mol) | 143.603 |
| SE (PM3) | (kcal/mol) | 137.889 |
| HF 3-21G(*) | (kcal/mol) | 145.893 |
| HF 6-31G* | (kcal/mol) | 148.375 |
| HF 6-31G** | (kcal/mol) | 111.512 |
| DF-B3LYP 6-31G* | (kcal/mol) | 123.39 |
| MP2 | (kcal/mol) | 87.448 |

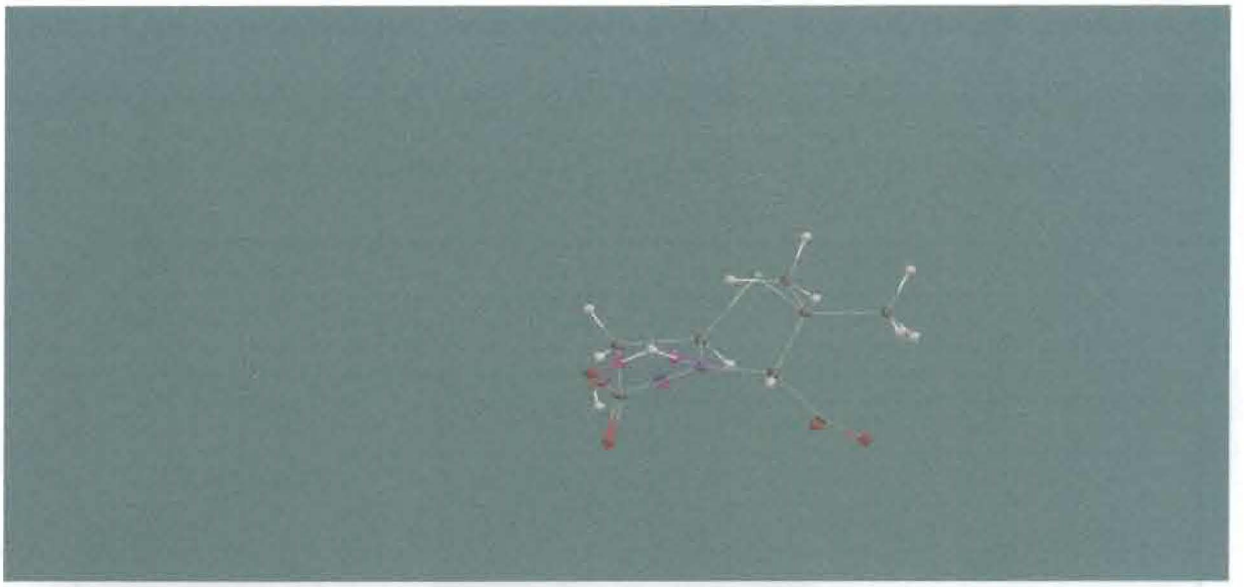

**Figure 12:** Optimized structure at B3LYP/6-31G* of β- lactam thiol ring with water at the transition state.

## B1b) Transition state of fused β- lactam thiol ring with water

**Table-13:** Shows computed values of ΔH of formation of reactants (water and fused β- lactam thiol ring) and transition state at different levels (with no $Zn^{2+}$).

| LEVEL OF THEORY | Units | ΔH of reactants | ΔH of transition state |
|---|---|---|---|
| SE (AM1) | (kcal/mol) | -169.581 | -63.791 |
| SE (PM3) | (kcal/mol) | -186.427 | -138.957 |
| HF 3-21G(*) | au | -1055.703435 | -1055.6877590 |
| HF 6-31G* | au | -1061.345792 | -1061.227282 |
| HF 6-31G** | au | -1061.374234 | -1061.2372824 |
| DF-B3LYP 6-31G* | au | -1065.930336 | -1065.8347250 |

Table- 14 shows activation energies at different levels of theory with no $Zn^{2+}$ present. Semi-empirical method gave the high value of $\Delta H^{\ddagger}$, and the activation energy steadily lowers as more functions are added to the HF basis set and DF-B3LYP at 6-31G* basis set.

**Table-14:** Activation energy of fused β- lactam thiol ring without zinc at various levels of theory.

| LEVEL OF THEORY | Units | Activation energy |
|---|---|---|
| SE (AM1) | (kcal/mol) | 105.79 |
| SE (PM3) | (kcal/mol) | 47.47 |
| HF 3-21G(*) | (kcal/mol) | 9.83 |
| HF 6-31G* | (kcal/mol) | 74.36 |
| HF 6-31G** | (kcal/mol) | 85.93 |
| DF-B3LYP 6-31G* | (kcal/mol) | 59.68 |

## B1c) Transition state of benzyl Penicillin with water

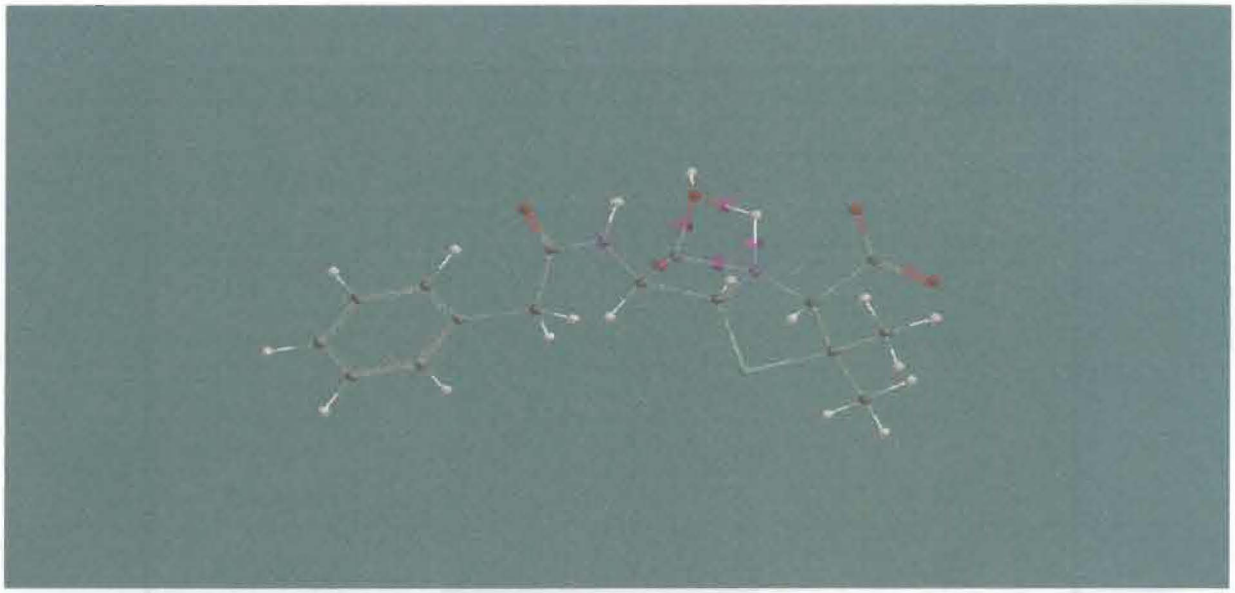

**Figure 13:** Optimized structure at B3LYP/6-31G* of benzyl Penicillin with water at the transition state.

**Table-15:** Shows computed values of ΔH of formation of reactants (water and benzyl Penicillin) and transition state at different levels (with no $Zn^{2+}$).

| LEVEL OF THEORY | Units | ΔH of reactants | ΔH of transition state |
|---|---|---|---|
| SE (AM1) | (kcal/mol) | -180.58 | -76.626 |
| SE (PM3) | (kcal/mol) | -197.785 | -159.301 |
| HF 3-21G(*) | au | -1489.711547 | -1489.6462470 |
| HF 6-31G* | au | -1497.723614 | -1497.5300310 |
| HF 6-31G** | au | -1497.753819 | -1497.562550 |
| DF-B3LYP 6-31G* | au | -1505.007586 | -1504.808125 |

**Table-16:** Activation energy of water and benzyl Penicillin without zinc at various levels of theory.

| LEVEL OF THEORY | Units | Activation energy |
|---|---|---|
| SE (AM1) | (kcal/mol) | 103.95 |
| SE (PM3) | (kcal/mol) | 38.484 |
| HF 3-21G(*) | (kcal/mol) | 40.97 |
| HF 6-31G* | (kcal/mol) | 121.47 |
| HF 6-31G** | (kcal/mol) | 122.76 |
| DF-B3LYP 6-31G* | (kcal/mol) | 125.16 |

## B2) Discussion:

The transition state (TS) is the highest point along the lowest energy pathway between reactants and products. It is very difficult to model transition state because unlike reactants and products, which are well defined entities, transition states are more distorted and their orbital are more diffused. Transition state may exhibit elongated bonds, partial bonding and some aspects of excited state. Transition state cannot easily be observed experimentally, so it is difficult to devise parameters to model them. Existence of a unique transition state is not clear. It is very difficult to predict its structure. Moreover the TS may involve partial bonding (very diffuse

unconventional orbitals) and so lower levels theory are not likely to help modeling. We also have kinetic and solvent effect data to help decide transition state geometries.

Based on the difficulties we followed an approach for predicting TS geometry. We first performed low level AM1 and PM3 semi-empirical MO calculation as a transition state structure, we used this result as a starting point for the higher level calculation as Hartree-Fock and density functional B3LYP at 6-31G* in Spartan 2004™. For the best energy optimization values we did the single point energy calculations and verified them with the frequency calculations at different levels.

We calculate the activation energy by taking the difference between ΔH (transition state) and ΔH (initial state). The lower level theory like AM1 did not give an adequate result, but PM3 yield high activation energy of approximately 38 to 104 kcal/mol. Hartree-Fock and density functional theories are in range of 40 to 125 kcal/mol.

The first step in the process is verification and confirmation of the transition structure. This involves the calculation of an energy profile. In energy profile calculations, characteristic bond lengths and bond angles are varied systematically from initial geometry to final product geometry, stepping each parameter incrementally along a single reaction coordinate by dividing its total change from reactant to product into equally spaced intervals. This is a concerted reaction mechanism where the critical bonds and angels all change synchronously.

## C) Building the transition state with enzyme: Introduction:

As per C. Prosperi-Meys, J. Wouters[2] et al. studied about the substrate binding and catalytic mechanism of class B β- lactamases. X-ray structures of several zinc β-lactamases have revealed the coordination of the two metal ions. Geometry optimization of stable complexes along the reaction pathway of benzyl Penicillin hydrolysis highlighted a proton shuttle occurring from D120 of the *Bacillus cereus* β- lactamases to the β- lactam nitrogen via Zn2 which is central to the network. First, the Zn1 ion has a structural role maintaining Zn-bound waters, WAT1 and WAT2, either directly or through the Zn1 tetrahedrally coordinated histidine ligands. Here we are using ammonia instead of histidine ligands.

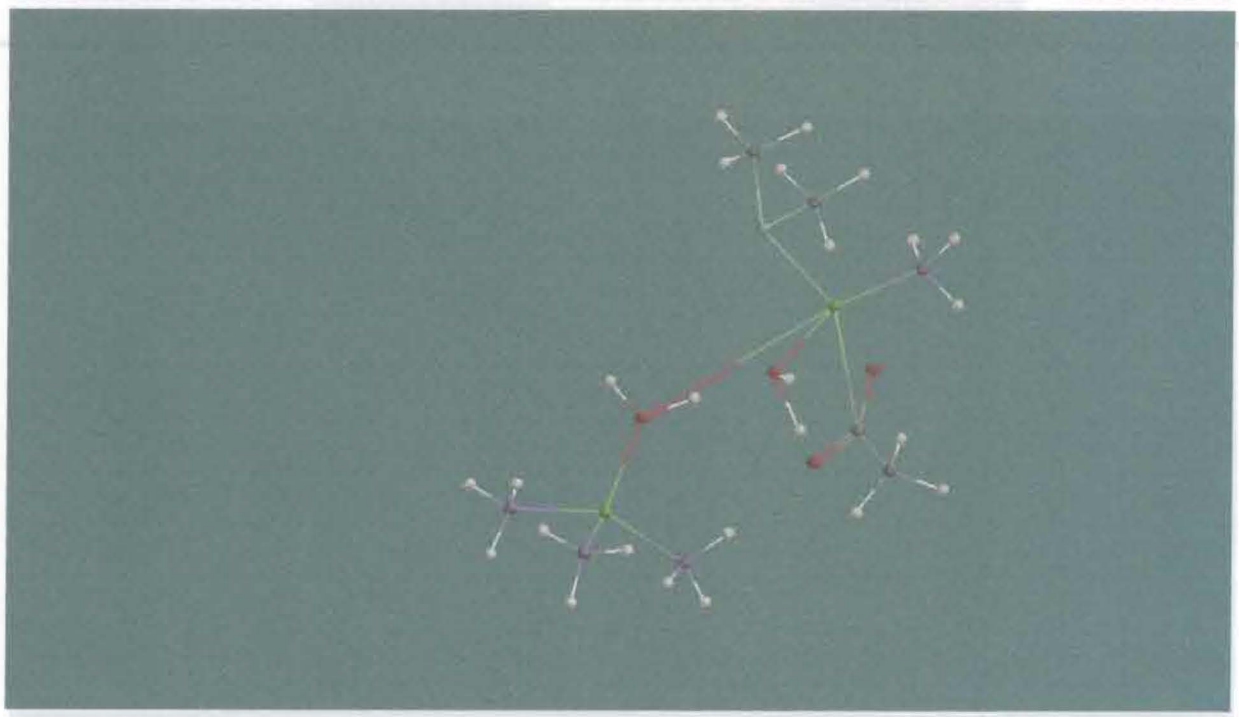

**Figure 14:** Optimized structure at B3LYP/6-31G* of β- lactamase enzyme (ammonia instead of histidine ligands).

## C1a) Building the transitional state with β- lactam ring and enzyme

**Table-17:** Heat of formation of β- lactam hydrolysis reaction with presence of enzyme.

| LEVEL OF THEORY | Units | Enzyme | β- lactam ring | Total |
|---|---|---|---|---|
| SE AM1 | (kcal/mol) | 332.825 | -21.849 | 310.97 |
| SE PM3 | (kcal/mol) | 14.42 | -21.849 | -7.429 |
| HF 3-21G(*) | au | -4613.1115984 | -244.4329365 | -4857.544535 |
| HF 6-31G* | au | -4635.2247297 | -245.8104325 | -4881.118579 |
| HF 6-31G** | au | -4635.3081466 | -245.8209986 | -4881.129145 |
| DF-B3LYP 6-31G* | au | -4643.1817234 | -247.2856180 | -4890.467341 |

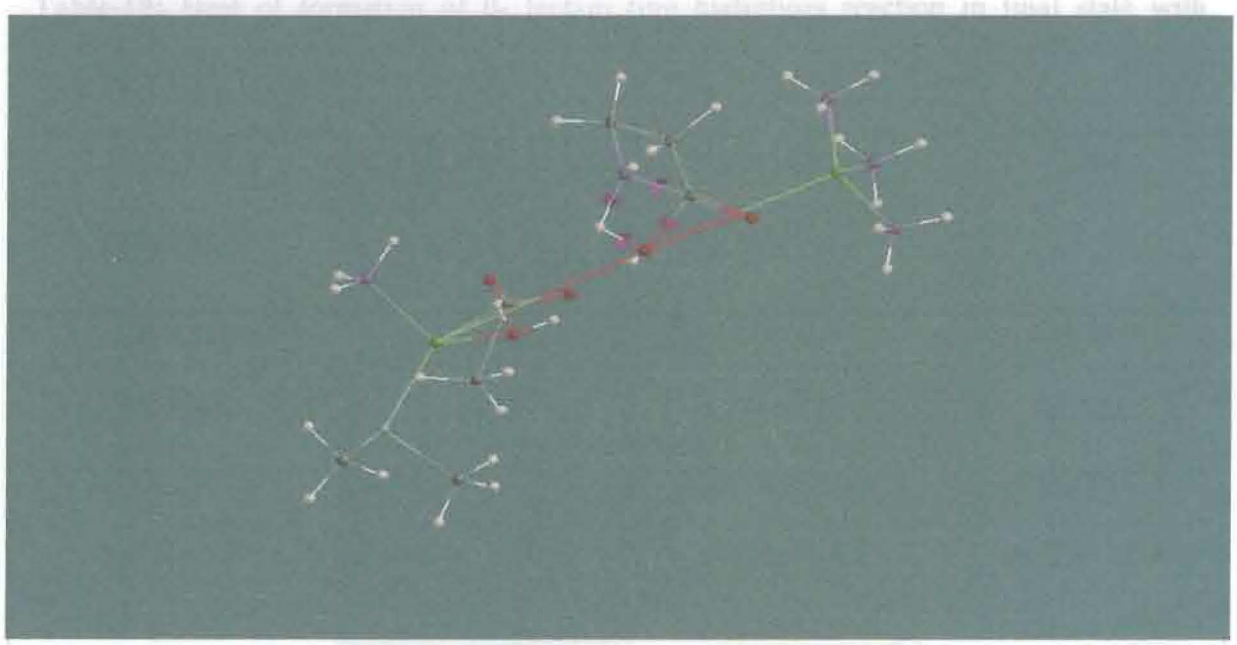

**Figure 15:** Optimized structure at B3LYP/6-31G* of β- lactam ring and β- lactamase enzyme, at the transition state.

**Table-18:** Heat of formation of β- lactam hydrolysis reaction in transition state with enzyme.

| LEVEL OF THEORY | Units | TS |
|---|---|---|
| SE AM1 | (kcal/mol) | 541.840 |
| SE PM3 | (kcal/mol) | 122.563 |
| HF 3-21G(*) | au | -4857.5541095 |
| HF 6-31G* | au | -4881.0312590 |
| HF 6-31G** | au | -4881.05792798 |
| DF-B3LYP 6-31G* | au | -4890.39429100 |

**Table-19:** Heat of formation of β- lactam ring hydrolysis reaction in final state with enzyme.

| LEVEL OF THEORY | Enzyme | Hydrolyzed β- lactam | Total |
|---|---|---|---|
| SE AM1 | 332.825 | -106.468 | 226.357 |
| SE PM3 | 14.42 | -99.5347 | -85.115 |
| HF 3-21G(*) | -4613.1115984 | -320.0701748 | -4933.181773 |
| HF 6-31G* | -4635.2247297 | -321.8675088 | -4957.092238 |
| HF 6-31G** | -4635.3081466 | -321.8876274 | -4957.195773 |
| DF-B3LYP 6-31G* | -4643.1817234 | -323.7384904 | -4966.920213 |

## C1b) Results:

**Table-20:** Computed values of ΔH of β- lactam ring reactants and transition state with zinc at different levels.

| LEVEL OF THEORY | Units | ΔH of reactants with zinc | ΔH of transition state with zinc |
|---|---|---|---|
| SE (AM1) | (kcal/mol) | 310.97 | 541.840 |
| SE (PM3) | (kcal/mol) | -7.429 | 122.563 |
| HF 3-21G(*) | au | -4857.544535 | -4857.5541095 |
| HF 6-31G* | au | -4881.118579 | -4881.0312590 |
| HF 6-31G** | au | -4881.129145 | -4881.05792798 |
| DF-B3LYP 6-31G* | au | -4890.467341 | -4890.39429100 |

Table- 20 shows computed activation energies with zinc at different levels of theories; comparison with table- 21 shows the dramatic lowering of the activation energy with zinc. Table- 22 contrasts both reactions.

**Table-21:** Computed activation energies with zinc in β- lactam ring at different levels of theory.

| LEVEL OF THEORY | Units | Activation energy with zinc |
|---|---|---|
| SE (AM1) | (kcal/mol) | 230.87 |
| SE (PM3) | (kcal/mol) | 130.0 |
| HF 3-21G(*) | (kcal/mol) | -------- |
| HF 6-31G* | (kcal/mol) | 54.79 |
| HF 6-31G** | (kcal/mol) | 44.69 |
| DF-B3LYP 6-31G* | (kcal/mol) | 45.83 |

When enzyme is included with reactants and transition state, the higher levels of theory gave consistent results with the activation energies ranging from 130 to 230 kcal/mol approximately on semi-empirical method and from 44.69 to 54.79 kcal/mol approximately Hatree-fock and density function theories. Zinc is clearly involved in the active site and participitates in reducing the activation energy. The computational effect of transition state with zinc is high and cannot be completely optimized. This serves as an excellent source of information for the further research on this reaction.

Table-22 shows computed activation energies with and without zinc and their difference. In general semi-empirical method (AM1) gave high values of activation energies both with and without zinc and lower reductions due to added zinc. The energy decreasing consistently as the density function basis set increase is due to the accounting for diffusion of electrons and distorted geometries.

**Table-22:** Activation energies with and without zinc in β- lactam ring kcal/mol.

| LEVEL OF THEORY | Activation energy (kcal) without zinc | Activation energy (kcal) with zinc | Reduction of $E_{act}$ due to catalysis |
|---|---|---|---|
| SE (AM1) | 143.60 | 230.87 | -------- |
| SE (PM3) | 137.88 | 130.0 | 7.88 |
| HF 3-21G(*) | 145.90 | ------- | --------- |
| HF 6-31G* | 111.51 | 54.79 | 56.72 |
| HF 6-31G** | 87.62 | 44.69 | 42.93 |
| DF-B3LYP 6-31G* | 87.44 | 45.38 | 42.06 |

## C2a) fused β- lactam thiol ring with enzyme

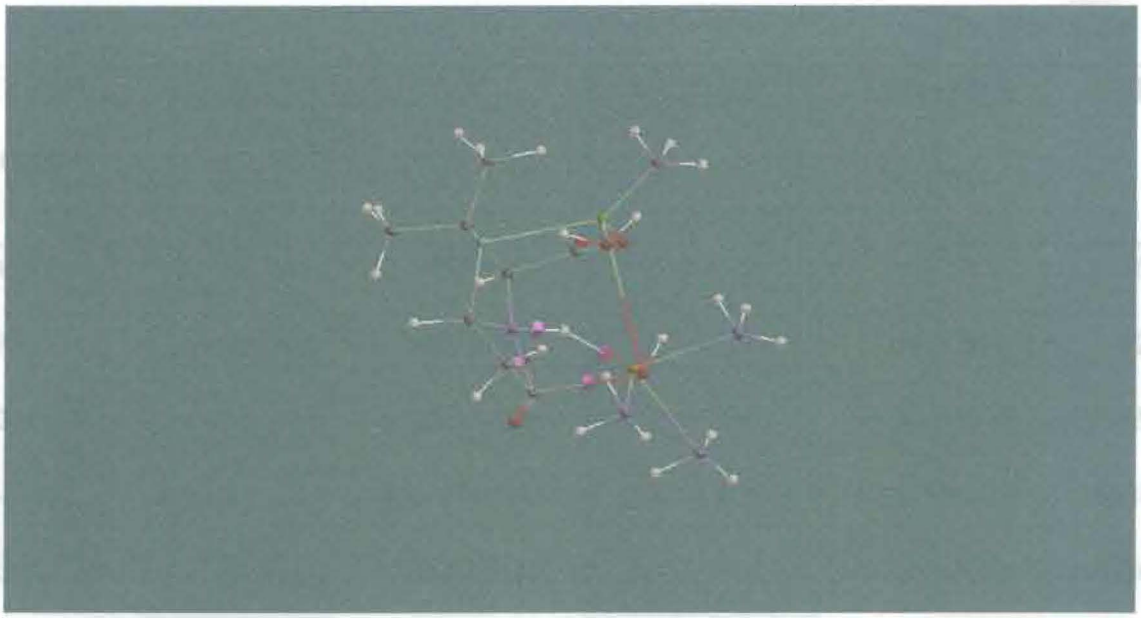

**Figure 16:** Optimized structure at B3LYP/6-31G* of fused β- lactam thiol ring and β-lactamase enzyme, at the transition state.

**Table-23:** Heat of formation of fused β- lactam thiol ring hydrolysis reaction with presence of enzyme.

| LEVEL OF THEORY | Units | Enzyme | β- lactam thiol ring | Total |
|---|---|---|---|---|
| SE AM1 | (kcal/mol) | 332.825 | -110.341 | 222.484 |
| SE PM3 | (kcal/mol) | 14.42 | -133.00 | -118.58 |
| HF 3-21G(*) | au | -4613.1115984 | -980.1174750 | -5593.229073 |
| HF 6-31G* | au | -4635.2247297 | -985.3350454 | -5620.559700 |
| HF 6-31G** | au | -4635.3081466 | -985.3506188 | -5620.658765 |
| DF-B3LYP 6-31G* | au | -4643.1817234 | -989.5213899 | -5632.703113 |

**Table-24:** Heat of formation of fused β- lactam thiol ring hydrolysis reaction in transition state with enzyme.

| LEVEL OF THEORY | Units | TS | ACET | Dimethyl Sulfate | Total |
|---|---|---|---|---|---|
| SE AM1 | (kcal/mol) | 383.908 | -115.4066 | -9.337 | 259.165 |
| SE PM3 | (kcal/mol) | 162.225 | 171.579 | -10.956 | 322.623 |
| HF 3-21G(*) | au | -4892.763700 | -225.9330679 | -474.456984 | -5593.1537521 |
| HF 6-31G* | au | -4916.519645 | -227.2250445 | -476.735334 | -5620.480023 |
| HF 6-31G** | au | -4916.600700 | -227.2298485 | -476.745005 | -5620.575553 |
| DF-B3LYP 6-31G* | au | -4926.137041 | -228.4978884 | -478.013864 | -5632.648793 |

**Table-25:** Heat of formation of fused β- lactam thiol ring hydrolysis reaction in final state with enzyme.

| LEVEL OF THEORY | Units | Enzyme | Hydrolyzed β- lactam thiol ring | Total |
|---|---|---|---|---|
| SE AM1 | (kcal/mol) | 332.825 | -217.647 | 115.178 |
| SE PM3 | (kcal/mol) | 14.42 | 218.197 | 232.617 |
| HF 3-21G(*) | au | -4613.1115984 | -1055.868753 | -5668.980351 |
| HF 6-31G* | au | -4635.2247297 | -1061.4168746 | -5696.641603 |
| HF 6-31G** | au | -4635.3081466 | -1061.4426871 | -5696.750833 |
| DF-B3LYP 6-31G* | au | -4643.1817234 | -1066.0061766 | -5709.187899 |

Table- 24 shows heat of formation of fused β- lactam thiol ring hydrolysis reaction in transition state with enzyme. We had the total heat of formation when we added all the molecules heat of formation. Table- 25 shows heat of formation of fused β- lactam thiol ring hydrolysis reaction in final state (product) with enzyme.

## C2b) Results:

**Table 26:** Computed values of ΔH of reactant and transition state in fused β- lactam thiol ring with zinc at different levels.

| LEVEL OF THEORY | Units | ΔH of reactants with zinc | ΔH of transition state with zinc |
|---|---|---|---|
| SE (AM1) | (kcal/mol) | 222.484 | 259.165 |
| SE (PM3) | (kcal/mol) | -118.58 | 322.623 |
| HF 3-21G(*) | au | -5593.229073 | -5593.1537521 |
| HF 6-31G* | au | -5620.559700 | -5620.480023 |
| HF 6-31G** | au | -5620.658765 | -5620.575553 |
| DF-B3LYP 6-31G* | au | -5632.703113 | -5632.648793 |

Table- 26 shows computed activation energies with zinc at different levels of theories; comparison with table- 27 shows the dramatic lowering of the activation energy with zinc. Table- 28 contrasts both reactions.

**Table-27:** Computed activation energies with zinc in $\beta$- lactam thiol ring at different levels of theory.

| LEVEL OF THEORY | Units | Activation energy with zinc |
|---|---|---|
| SE (AM1) | (kcal/mol) | 36.681 |
| SE (PM3) | (kcal/mol) | 441.203 |
| HF 3-21G(*) | (kcal/mol) | 47.26 |
| HF 6-31G* | (kcal/mol) | 49.99 |
| HF 6-31G** | (kcal/mol) | 52.21 |
| DF-B3LYP 6-31G* | (kcal/mol) | 34.08 |

When enzyme is included with reactants and transition state, the higher levels of theory gave consistent results with the activation energies ranging from 36.7 to 441.2 kcal/mol approximately on semi-empirical method, and from 34.08 to 52.21 kcal/mol approximately on Hatree-fock and density function theories. Zinc is clearly involved in the active site and participitates in reducing the activation energy. The computational effect of transition state with zinc is high and cannot be completely optimized. This serves as an excellent source of information for the further research on this reaction.

Table-28 shows computed activation energies with and without Zinc and their difference. In general semi-empirical method (AM1) gave high values of activation energies without zinc and lower reductions due to added zinc and HF 3-21G (*) and PM3 are giving in negative values. The energy decreasing consistently as the density function basis set increase is due to the accounting for diffusion of electrons and distorted geometries.

**Table-28:** Activation energies in fused β- lactam thiol ring with and without zinc kcal/mol.

| LEVEL OF THEORY | Activation energy (kcal) without zinc | Activation energy (kcal) with zinc | Reduction of $E_{act}$ due to catalysis |
|---|---|---|---|
| SE (AM1) | 105.79 | 36.681 | 69.109 |
| SE (PM3) | 47.47 | 441.203 | -------- |
| HF 3-21G(*) | 9.83 | 47.26 | -------- |
| HF 6-31G* | 68.09 | 49.99 | 18.10 |
| HF 6-31G** | 85.94 | 52.21 | 33.73 |
| DF-B3LYP 6-31G* | 59.11 | 34.08 | 25.03 |

## C3a) Benzyl Penicillin with enzyme

**Table-29:** Heat of formation of benzyl Penicillin hydrolysis reaction with presence of enzyme.

| LEVEL OF THEORY | Units | Enzyme | Benzyl Penicillin | Total |
|---|---|---|---|---|
| SE AM1 | (kcal/mol) | 332.825 | -121.34 | 221.482 |
| SE PM3 | (kcal/mol) | 14.42 | -144.35 | -129.94 |
| HF 3-21G(*) | au | -4613.1115984 | -1414.1255871 | -6027.237185 |
| HF 6-31G* | au | -4635.2247297 | -1421.6999999 | -6056.924728 |
| HF 6-31G** | au | -4635.3081466 | -1421.7302047 | -6057.038350 |
| DF-B3LYP 6-31G* | au | -4643.1817234 | -1428.596400 | -6071.780363 |

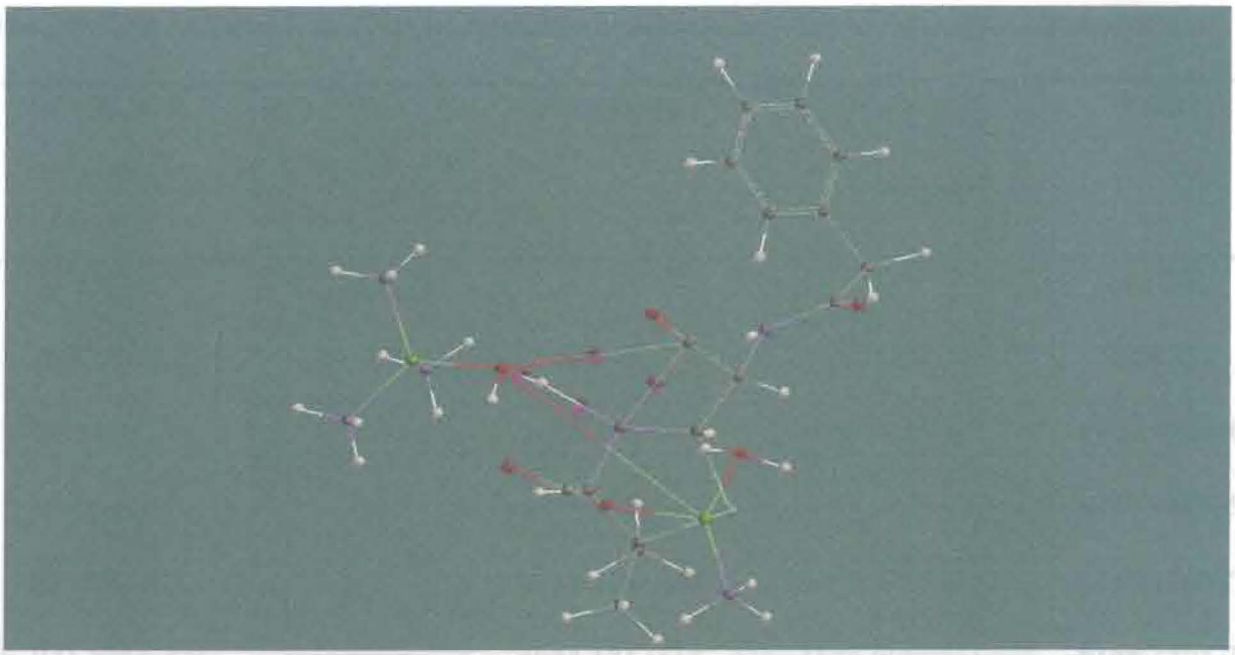

**Figure 17:** Optimized structure at B3LYP/6-31G* of benzyl Penicillin and β- lactamase enzyme, at the transition state.

**Table-30:** Heat of formation of benzyl Penicillin hydrolysis reaction in transition state with enzyme.

| LEVEL OF THEORY | Units | TS | ACET | Dimethyl Sulfate | TOTAL |
|---|---|---|---|---|---|
| SE AM1 | (kcal/mol) | 432.390 | -115.4066 | -9.337 | 307.64 |
| SE PM3 | (kcal/mol) | 118.096 | 171.579 | -10.956 | 278.704 |
| HF 3-21G(*) | au | -5326.74057 | -225.933067 | -474.456984 | -6027.13063 |
| HF 6-31G* | au | -5354.78993 | -227.225044 | -476.735334 | -6028.73779 |
| HF 6-31G** | au | -5352.88881 | -227.229848 | -476.745005 | -6056.44479 |
| DF-B3LYP 6-31G* | au | -5365.08949 | -228.497888 | -478.013864 | -6071.60125 |

**Table-31:** Heat of formation of benzyl Penicillin hydrolysis reaction in final state with enzyme.

| LEVEL OF THEORY | Units | Enzyme | Hydrolyzed Benzyl Penicillin | Total |
|---|---|---|---|---|
| SE AM1 | (kcal/mol) | 332.825 | -223.92 | 108.905 |
| SE PM3 | (kcal/mol) | 14.42 | 231.70 | 246.12 |
| HF 3-21G(*) | au | -4613.1115984 | -1489.8010224 | -6102.912620 |
| HF 6-31G* | au | -4635.2247297 | -1497.7717631 | -6132.099649 |
| HF 6-31G** | au | -4635.3081466 | -1497.8122914 | -6133.120437 |
| DF-B3LYP 6-31G* | au | -4643.1817234 | -1505.0650973 | -6148.246820 |

## C3b) Results:

**Table 32:** Computed values of ΔH of reactant and transition state with zinc in benzyl Penicillin hydrolysis reaction at different levels.

| LEVEL OF THEORY | Units | ΔH of reactants with zinc | ΔH of transition state with zinc |
|---|---|---|---|
| SE (AM1) | (kcal/mol) | 221.482 | 307.64 |
| SE (PM3) | (kcal/mol) | -129.94 | 278.704 |
| HF 3-21G(*) | au | -6027.237185 | -6027.13063 |
| HF 6-31G* | au | -6056.924728 | -6028.73779 |
| HF 6-31G** | au | -6057.038350 | -6056.44479 |
| DF-B3LYP 6-31G* | au | -6071.780363 | -6071.60125 |

Table- 32 shows computed activation energies with zinc at different levels of theories; comparison with table- 33 shows the dramatic lowering of the activation energy with zinc. Table- 34 contrasts both reactions.

**Table-33:** Computed activation energies with zinc in benzyl Penicillin hydrolysis reaction at different levels of theory.

| LEVEL OF THEORY | UNITS | Activation energy with zinc |
|---|---|---|
| SE (AM1) | (kcal/mol) | 86.158 |
| SE (PM3) | (kcal/mol) | 408.640 |
| HF 3-21G(*) | (kcal/mol) | 66.86 |
| HF 6-31G* | (kcal/mol) | 109.42 |
| HF 6-31G** | (kcal/mol) | 109.60 |
| DF-B3LYP 6-31G* | (kcal/mol) | 112.39 |

When enzyme is included with reactants and transition state, the higher levels of theory gave consistent results with the activation energies ranging from 86.158 to 408.6 kcal/mol approximately on semi-empirical method and from 66.86 to112.39 kcal/mol approximately on Hatree-fock and density function theories. Zinc is clearly involved in the active site and participitates in reducing the activation energy. The computational effect of transition state with zinc is high and cannot be completed optimization. This serves as an excellent source of information for the further research on this reaction.

Table- 33 shows computed activation energies with and without zinc and their difference. In general semi-empirical method (PM3) gave very high values of activation energies with and gave without zinc, and greater reductions due to added zinc. The energy decreasing consistently as the density function basis set increases is due to the accounting for diffusion of electrons and distorted geometries.

**Table-34:** Activation energies with and without zinc.

| LEVEL OF THEORY | Activation energy (kcal) without zinc | Activation energy (kcal) with zinc | Reduction of $E_{act}$ due to catalysis |
|---|---|---|---|
| SE (AM1) | 103.96 | --------- | ---------- |
| SE (PM3) | 38.48 | ---------- | ---------- |
| HF 3-21G(*) | -40.78 | 66.86 | ---------- |
| HF 6-31G* | 121.47 | 109.60 | 11.87 |
| HF 6-31G** | 122.76 | 109.60 | 13.16 |
| DF-B3LYP 6-31G* | 125.16 | 112.39 | 12.77 |

## D) Metal ion effect:

Geometry optimization of stable complexes along the reaction pathway of benzyl Penicillin hydrolysis highlighted a proton shuttle occurring from D120 of the *Bacillus cereus* β- lactamases to the β- lactam nitrogen via Zn2 which is central to the network. First, the Zn1 ion has a structural role maintaining Zn-bound waters, WAT1 and WAT2, either directly or through the Zn2 tetrahedrally coordinated histidine ligands. The Zn1 ion

has a more catalytic role, stabilizing the tetrahedral intermediate, accepting the β- lactam nitrogen atom as a ligand. The role of Zn 2 and the flexibility in the coordination geometry of both Zn ions is of crucial importance for catalysis. One of our goals is to establish zinc ions catalytic activity by modeling that it reduces the activation energy.

## E) Product confirmation:

After the calculations of activation energies, we confirmed that the actual product formed from the activated complex by comparing the bond length of these products by their experimental values. The values were also used to give a more detailed picture of the reaction.

Benzyl Penicillin hydrolysis reaction energies for initial (IS), transition state (TS), and final state (FS) are calculated based in isolated molecules. The reaction coordinate (q) contains all critical coordinates stepped proportionally.

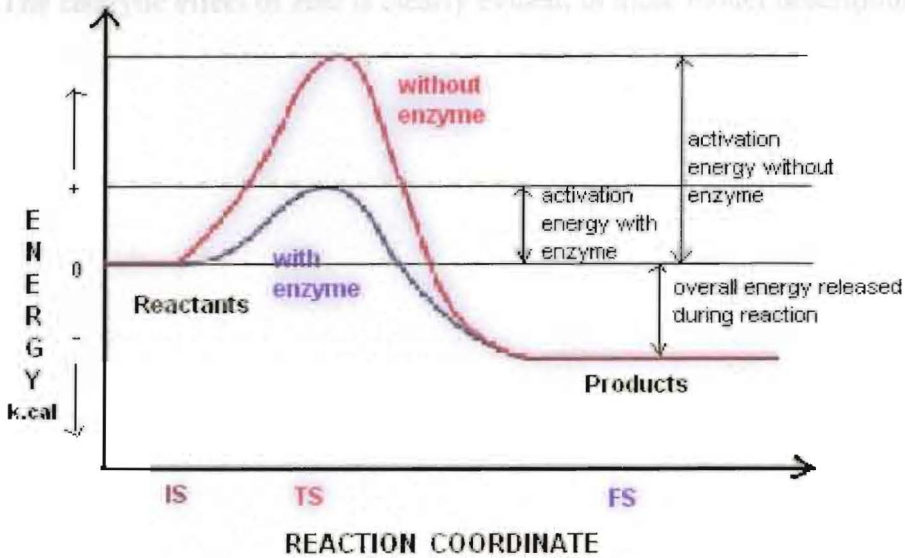


**Figure-18:** Energy profile of zinc ion catalyzed and uncatalyzed minimal benzyl Penicillin hydrolysis reaction.

## E1) DISCUSSION:

We had calculated equilibrium geometries of this initial sate, corresponding to isolated but close reactants, with success in convergence. The next step is to predict the transition state structure and its optimization by calculating transition state geometry. Another set of difficulties related to their incorporation of partial bonds. When the numbers of bonding and non-bonding electron pairs are changing, very large basis sets and significant inclusion of electron correlation are required for accurate description. If one is attempting to use a semi-empirical MO method, one should be particularly concerned that these methods were empirically parameterized for stable molecules, and thus are much less likely to perform well in describing transition structures. The successful convergence and optimization the bond-lengths of the transition state are noted in the table. The product bond lengths can be calculated from the isolated product molecules or the reaction profile calculations. The catalytic effect of zinc is clearly evident in these model descriptions.

# CHAPTER 4

## Conclusion:

In an attempt to model the active site of benzyl penicillin hydrolysis reaction, we investigated the relevant thermodynamics and kinetics of this mechanism and the transition state of various basis sets. After gaining confidence that these models were suitable for ground states, we computed transition state energies and geometries, and examined the particular role of a zinc ion in reducing the activation energy. We can see that only the semi-empirical AM1 method gave very high $E_a$.

**Table-35:** Activation energies in $\beta$- lactam ring with and without zinc (kcal/mol).

| LEVEL OF THEORY | Activation energy (kcal) without zinc | Activation energy (kcal) with zinc | Reduction of $E_{act}$ due to catalysis |
|---|---|---|---|
| SE (AM1) | 143.60 | 230.87 | --------- |
| SE (PM3) | 137.88 | 130.0 | 7.88 |
| HF 3-21G(*) | 145.90 | ------- | --------- |
| HF 6-31G* | 111.51 | 54.79 | 56.72 |
| HF 6-31G** | 87.62 | 44.69 | 42.93 |
| DF-B3LYP 6-31G* | 87.44 | 45.38 | 42.06 |

**Table-36:** Activation energies in β- lactam thiol ring with and without zinc (kcal/mol).

| LEVEL OF THEORY | Activation energy (kcal) without zinc | Activation energy (kcal) with zinc | Reduction of $E_{act}$ due to catalysis |
|---|---|---|---|
| SE (AM1) | 105.79 | 36.681 | 69.109 |
| SE (PM3) | 47.47 | 441.203 | -------- |
| HF 3-21G(*) | 9.83 | 47.26 | -------- |
| HF 6-31G* | 68.09 | 49.99 | 18.10 |
| HF 6-31G** | 85.94 | 52.21 | 33.73 |
| DF-B3LYP 6-31G* | 59.11 | 34.08 | 25.03 |

**Table-37:** Activation energies in benzyl Penicillin with and without zinc (kcal/mol).

| LEVEL OF THEORY | Activation energy (kcal) without zinc | Activation energy (kcal) with zinc | Reduction of $E_{act}$ due to catalysis |
|---|---|---|---|
| SE (AM1) | 103.96 | -------- | ---------- |
| SE (PM3) | 38.48 | --------- | ---------- |
| HF 3-21G(*) | -40.78 | 66.86 | ---------- |
| HF 6-31G* | 121.47 | 109.60 | 11.87 |
| HF 6-31G** | 122.76 | 109.60 | 13.16 |
| DF-B3LYP 6-31G* | 125.16 | 112.39 | 12.77 |

These activation energy values are lower limits since the initial state configuration, though the same for all methods brought the oppositely charged reactants near to β- lactam ring geometry. The clear catalytic role of zinc is manifested.

For the concerted one step benzyl Penicillin hydrolysis reaction energy profile was computed as a function of normalized bond-length changes to reflect all these changes in a single reaction coordinate, from reactants to products. This was constructed using B3LYP/6-31G* (density functional theory) since it gives nearly the lowest value for the activation energy in the high level of theories. The density functional theory adds in electron repulsions without excited states.

Finally we attempted to stimulate the active site of β- lactamase itself. The biological active site is simplified by using imidazole rings in the place of histidine to make the computation practical we used B3LYP/6-31G* to model this, but we did not succeed due to low processing computer. For computing these high level theories for such big molecules we need a very high processing computer with high memory, with that we can most likely see the charge distribution due to the zinc ions in the transition state. It could be added that the computation times required for various levels of theory and basis sets range from a few minutes to 15 days approximately. Accurate thermodynamic results could be obtained quickly in lower level of semi-empirical theories, but higher level theories like Hartree-Fock and density functional theory we need a very high processing computer. In transition states it took much longer time for giving the optimization energy steps.

# CHAPTER 5

## Future work:

Besides modeling enzyme-substrate interactions in biochemical conversions like β-lactamase hydrolysis reaction, many other applications of modeling to bimolecular systems are possible for β- lactamase hydrolysis reaction. We should simulate the other more complex active sites in the normal system.

Since almost all the fundamental advances have to date stemmed from investigations on the secondary metabolites of micro-organisms, it is reasonable to suppose that detailed examination of nature's resources may well provide further gains in terms of new β- lactam systems which will, then, require fine tuning by medicinal chemists.

Considerable ingenuity and effort has already been, and undoubtedly will continue to be, expended on the modification of the known natural β- lactam systems to improve their anti-bacterial spectrum or to render them stable to the various hydrolytic enzymes.

It is a hope that crystallographic structure analysis of β- lactamase information, coupled with the advances in the computer modeling of molecular interactions, will enable the more rational design to novel β- lactams and perhaps even non-β- lactam systems with both anti-bacterial and β- lactamase inhibitory activity.

## 9) Bibliography:


1) Fleming, A. (1929). *Br. J. Exp. Path.* 10, 226-236.

2) Morin, R. B.; Gorman, M., eds. (1982) "Chemistry and Biology of Beta-Lactam Antibiotics"Academic Press, London.

3) C.Prosperi-Meys, J.Wouters, M.Galleni, and J.Lamotte-Brasseur, *CMLS, Cell. Mol. Life Sci.* **2001** 58, 2136-2143.

4) Hehre, W.J.; Ditchfield, R. and Pople, J. A. *J.Chem.Phys.***1972**, 56, 2257.

5) Natalia Diaz, Dimas Suarez and Kenneth M.Merz, Jr, *J.Am.Chem.Soc.***2001**, 123, 9867-9879.

6) Binkley, J.S.; Pople,J.A. and Hehre, W.J. *J.Chem Soc.***1980**, 102,939.

7) Leach, A.R., "Molecular modeling:Principles and Applications,"2nd ed., Pearson Prentice Hall,Harlow,England; **2001.**

8) Becke, A. D. *J. Chem. Phys* ,**1993**, 98, 1372.

9) Stewart, J.J.P.*J.Computational Chem*, **1989**, 10,209.

10) Hehre, W.J.; Stewart.R. F.; and Pople, J. A, *J.Chem.Phys.* **1996,** 51, 2657.

11) Barrie W.Bycroft and Richard E.Shute, *Pharmaceutical Research*, **1985.**